Applied Energy 357 (2024) 122484

Contents lists available at ScienceDirect

Applied Energy

journal homepage: www.elsevier.com/locate/apenergy

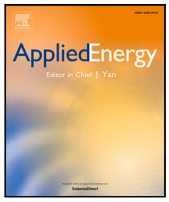

Hydrogen for harvesting the potential of offshore wind: A North Sea case study

Espen Flo Bødal [a,*], Sigmund Eggen Holm [a], Avinash Subramanian [a], Goran Durakovic [a,b], Dimitri Pinel [a], Lars Hellemo [c], Miguel Muñoz Ortiz [c], Brage Rugstad Knudsen [a], Julian Straus [a]

[a] SINTEF Energy Research, Kolbjørn Hejes vei 1B, 7491, Trondheim, Norway
[b] Department of Industrial Economics and Technology Management, Norwegian University of Science and Technology, Trondheim, Norway
[c] SINTEF Industry, P.O. Box 4760, Torgarden, 7465, Trondheim, Norway

ARTICLE INFO

Dataset link: Data for: "Hydrogen for harvesting the potential of offshore wind: A North Sea case study" (Original data)

Keywords:
Offshore wind
Electrolysis
Energy export
Decarbonisation

ABSTRACT

Economical offshore wind developments depend on alternatives for cost-efficient transmission of the generated energy to connecting markets. Distance to shore, availability of an offshore power grid and scale of the wind farm may impede export through power cables. Conversion to H_2 through offshore electrolysis may for certain offshore wind assets be a future option to enable energy export. Here, we analyse the cost sensitivity of offshore electrolysis for harvesting offshore wind in the North Sea using a technology-detailed multi-carrier energy system modelling framework for analysis of energy export. We include multiple investment options for electric power and hydrogen export including HVDC cables, new hydrogen pipelines, tie-in to existing pipelines and pipelines with linepacking. Existing hydropower is included in the modelling, and the effect on offshore electrolysis from increased pumping capacity in the hydropower system is analysed. Considering the lack of empirical cost data on offshore electrolysis, as well as the high uncertainty in future electricity and H_2 prices, we analyse the cost sensitivity of offshore electrolysis in the North Sea by comparing costs relative to onshore electrolysis and energy prices relative to a nominal scenario. Offshore electrolysis is shown to be particularly sensitive to the electricity price, and an electricity price of 1.5 times the baseline assumption was needed to provide sufficient offshore energy for any significant offshore electrolysis investments. On the other hand, too high electricity prices would have a negative impact on offshore electrolysis because the energy is more valuable as electricity, even at the cost of increased wind power curtailment. This shows that there is a window-of-opportunity in terms of onshore electricity where offshore electrolysis can play a significant role in the production of H_2. Pumped hydropower increases the maximum installed offshore electrolysis at the optimal electricity and H_2 prices and makes offshore electrolysis more competitive at low electricity prices. Linepacking can make offshore electrolysis investments more robust against low H_2 and high electricity prices as it allow for more variable H_2 production through storing excess energy from offshore. The increased electrolysis capacity needed for variable electrolyser operation and linepacking is installed onshore due to its lower CAPEX compared to offshore installations.

1. Introduction

Offshore wind has a massive, global potential for renewable electricity generation and is a key technology for enabling the scale of renewable electricity generation necessary to accelerate the energy transition [1,2]. Following the Paris Agreement of 2015 [3], the European Union (EU) signed the European Green Deal [4], setting the goal of cutting greenhouse gas (GHG) emissions with 55% compared to 1990 levels by 2030, and becoming carbon neutral by 2050. The EU offshore energy strategy [5] reiterates offshore wind as a central point to reach the climate goals.

New, massive development plans for offshore wind are frequently heralded both by authorities and energy industries in countries with large coastlines and energy industries. The total installed capacity of offshore wind in Europe (including, *e.g.*, the United Kingdom) is now approaching 30 GW, with an average of approximately 3 GW installed per year for the past five years [6]. Due to the increased development of offshore wind farms, the global weighted average levelized cost of electricity (LCOE) has decreased by 13% in the period 2010–2017 and is therefore competitive with other renewable sources [7].

* Corresponding author.
E-mail address: espen.bodal@sintef.no (E.F. Bødal).

https://doi.org/10.1016/j.apenergy.2023.122484
Received 31 May 2023; Received in revised form 24 November 2023; Accepted 10 December 2023
Available online 16 December 2023

Furthermore, the capital expenditures (CAPEX) of projects commissioned after 2020 is expected to reduce a further 22% compared to the period 2013–2017 [7]. However, in the latest report on climate change, the IPCC stated that the current deployment of renewable energy is still insufficient to meet climate goals [8]. Offshore wind energy is therefore expected to continue growing, with European governments pledging to further add up to 160 GW of offshore wind by 2030 [6], where the ambitions of the EU (excluding, *e.g.*, the United Kingdom), is to increase the capacity from 12 GW today to at least 60 GW by 2030 [9].

As the share of intermittent energy sources in the energy system like wind power increases, so does the need for increased flexibility. It is also desirable to reduce curtailment for maximum utilisation of the turbines, thereby increasing their value. Pumped hydro and flexible hydrogen (H_2) production from electrolysis coupled with storage are two sustainable alternatives for serving this purpose. The development of pumped hydro requires existing dams with downstream reservoirs for reasonable investment costs and a reduced impact on nature. Hence, closed-loop off-river pumped hydro has been shown to have a significant global potential for supporting energy systems with large-scale developments of intermittent renewable energy sources [10].

Given the proper infrastructure, H_2 could also be an attractive energy carrier in the future. Even though H_2 has a low volumetric energy density, it has a high mass energy density when compared to other decarbonised alternatives such as batteries. Therefore, H_2 is seen as an attractive energy carrier in hard-to-abate sectors such as long-distance road transport, shipping and high-temperature industrial heating, where denser energy carriers are needed [11,12].

The initial development of offshore wind has been centred around the best projects close to shore, but as the development of offshore wind continues more difficult and expensive resources will have to be accessed farther from shore and at greater depths. One of the major costs of remote offshore wind is grid connection and transmission to the market through high voltage direct current (HVDC) cables [13], which require large capital investments that are sensitive to both distance and capacity [14]. In a market with a H_2 demand, the production of H_2 from offshore wind could have several benefits. Offshore H_2 production can provide local flexibility offshore, leading to less curtailment and greater capacity utilisation of both wind turbine and HVDC capacity. When large amounts of energy are transmitted, pipelines are an order of magnitude less costly for each unit of energy transported compared to HVDC lines. Given that there are sufficient H_2 end-users to create a large-scale demand, offshore electrolysis and H_2 pipelines could reduce the needed capacity of HVDC cables. In turn, the energy from offshore wind can be extracted at scale from remote location at lower cost and curtailment. It is previously shown in a study on the connection of energy islands in the North Sea and Baltic Sea by Lüth et al. [15] that transport of the energy as H_2 is beneficial for wind farms that are located far from shore. Using pipelines to transport H_2 produced offshore by electrolysis, either newly built or existing, may cause gas-flow fluctuations and thereby less continuous pipeline operations due to the intermittency of the renewable generation. This challenge can be mitigated if H_2 storage is developed, the renewable generation capacity is large, or if offshore and onshore produced H_2 share pipeline infrastructure for export.

H_2 has been used on a large scale in industrial processes for a century [16]. Even though thousands of km of H_2 pipelines currently exist, all are onshore and offshore H_2 pipelines so far lack industrial standardisation [16]. The main challenge with the design of H_2 pipelines is to overcome H_2 embrittlement and leakages [17]. Re-purposing of existing offshore natural gas pipelines is another alternative to constructing new dedicated H_2 pipelines [16].

A multitude of studies have analysed the integration of offshore wind or other intermittent energy sources in the energy system. Electrification and decarbonisation of oil and gas platforms in the North Sea have been widely studied [18–20]. Many studies analyse some form of power link islands or different concepts of offshore energy hubs in the North Sea [18,20,21]. In this paper, we consider an offshore energy hub to be a platform or island where H_2 can be produced on a large scale and, at the same, time function as a connection point for power cables from neighbouring countries or offshore wind farms. It can also serve as a junction for pipelines carrying H_2. Several studies investigated onshore or offshore H_2 production for increasing flexibility and reducing curtailment [21–27]. In an economic assessment of onshore electrolysis based on power from offshore wind farms in the Irish Sea, McDonagh et al. [22] found H_2 production for lowering curtailment to be economically viable only if they can achieve a H_2 price of at least 3.70 €/kg. Using a mixed-integer linear program (MILP) model, offshore electrolysis was found to lead to higher cost for the overall energy system, but with the flexibility of H_2 storage in offshore caverns, the potential was more promising [23]. Contrary, Singlitico et al. [21] found that producing H_2 offshore results in the lowest cost H_2. They also found a 13% reduction of LCOE with electrolysers in the system when compared to the LCOE in a system without electrolysers. In a study on how H_2 investments affect grid infrastructure and power prices, Durakovic et al. [24] found that energy hubs are important for the development of offshore wind in the North Sea and that the production of green H_2 significantly reduced the curtailment of offshore wind. However, the study also found that large-scale H_2 production cannot solely rely on otherwise curtailed renewable energy generation, and the energy demand for H_2 production leads to an increased European power generation capacity of around 50%. Onshore production of H_2 from offshore wind in Germany was studied by Scolaro and Kittner [25]. This study found that the lowest cost of H_2 occurs when the installed electrolyser capacity is at 87% of the wind farm capacity. They also found that participating in the ancillary service market is key for profitable H_2 production. Onshore H_2 production in Europe was also considered by Gawlick and Hamacher [26]. They found that given the availability of cheap large scale H_2 storage in e.g. salt caverns, H_2 production can decrease the vast needs for electricity storage and transmission capacity when the shares of wind and solar energy increases. Lucas et al. [27] performed a techno-economic study of potential onshore H_2 production from otherwise curtailed offshore wind in Portugal. The study found that the economic feasibility of such a project is highly dependent on a long-term commercial phase where an existing H_2 distribution network by pipelines is assumed. In a techno-economic study [28] on a H_2-supply chain, H_2 transport by a long-distance pipeline was studied. A long-distance H_2-pipeline was also central in the study of Sens et al. [29] where cost-optimal locations for green H_2 production for the European market were sought. Neither of the studies modelled the effect of linepacking in H_2-pipelines, which was found to be a research gap in energy system models [30]. In He et al. [31], a linear optimisation model was built to analyse a local H_2 supply chain, with a focus on modelling flexible transport as trucks and pipelines with linepacking. Due to the reduced need for trucks and storage, a significant cost reduction was found. Quarton and Samsatli [32] performed a more detailed modelling of linepacking in a MILP and studied blending of H_2 in a natural gas pipeline network. They found that with pure H_2-pipelines, the flexibility of the system is reduced to 17–26% of the equivalent value with natural gas. This is due to the lower energy density and compressibility of H_2.

The main contributions of this paper can be summarised as:

- systematically analysing the necessary conditions for offshore electrolysis in terms of CAPEX, onshore electricity and onshore H_2 price; and
- the impact of ability of feed-in into an existing H_2 pipeline, pumped hydro and line packing variations, on the economic feasibility of electrolysis offshore compared to onshore.

The paper is structured as follows; the methodology is explained in Section 2, this methodology is applied on the North Sea case study which is outlined in Section 3. Results from the case study are presented in Section 4, which create the foundation for the discussion in Section 5. The final conclusions are drawn in Section 6.

2. Method

2.1. Model structure

EnergyModelsX.[1] is a capacity expansion model with multiple energy carriers, developed to study the development and increasing interaction of large-scale energy systems. The model is written in the `Julia` programming language using the JuMP modelling framework [33]. This enables fast computing and a modular modelling framework by taking advantage of `Julia`'s multiple dispatch feature. The modularity enables users to select the appropriate technology and spatial representation based on the study to be conducted. This study is the first application of the model.

The model consists of two fundamental packages, the base package and the time package. Simple and generic representations of different technologies are defined in the base package, such as sink, source, generation, storage and links between these technologies. The base package also defines products, which can be used to represent any energy carrier, emission or general resource. The user interface is based on setting up the energy system as a graph, and the appropriate constraints are set based on the technology nodes used. Therefore, implementing a new technology only amounts to writing the general constraints for a node of the new type by overriding existing methods. The time package defines the time structure of the model independent of the technology representation. The time structure allows for varying the number and length of strategic and operational periods.

The base package can be extended with a geographical representation. This is done by defining areas as local energy systems. The individual areas are connected through transmission links, which are associated with transmission modes to enable the conveyance of selected resources between the areas. These transmission modes can, for example, be HVDC power lines or H_2 pipelines. Each area is connected to a local core node, which keeps track of the energy or mass balances of each resource in the local system and how it is exchanged with other areas. Within a local system, smaller energy sub-systems can be implemented as well. For example, wind power can be connected directly to the core node or exclusively to electrolysis, which is then connected to the core node. The modularity of the model allows for extending or re-implementing the technical details of a node or transmission mode without making changes in the base packages.

Running the model as an operational model is the default. Then, the objective function minimises the operational costs. However, investments in different technologies and transmissions can optionally be activated. Such that the objective function minimises the discounted operational and investment costs (see the details in Appendix B.4.1).

2.2. Modelling

In the developed framework *EnergyModelsX*, products are represented with the index p. These can be energy carriers of different kinds, emissions or resources used in production. Technology nodes are represented by the index n and are connected in a network with links l to represent the desired infrastructure as a directed graph.

The model uses a two-level time structure. Let $\mathcal{T}$ be a set of time steps $t_{i,j}$ indexed by the strategic period i and the operational period j. The set $\mathcal{T}^{\text{Inv}}$ denotes the collection of investment periods t_i. In some places, an investment period $t_i = t^{\text{inv}}$ will denote the set containing all operational periods $t_{i,j}$, but this will be clear from the context. The first strategic period will thus be denoted by t_0 and the first operational period of any investment period is denoted by $t_{i,0}$. The length of the operational period t is denoted by Δt, and correspondingly for an investment period Δt^{inv}. To simplify the notation in certain places, the operational period prior to $t = t_{i,j}$, will be denoted by $t - 1 = t_{i,j-1}$. Similarly, for strategic periods, we let $t_i - 1 = t_{i-1}$.

Below, we provide a comprehensive technology description of a pipeline with linepacking and a hydropower node, as these components will be critical to the analysis. We refer to Appendix B for the complete model description. All symbols are listed and explained in Appendix A.

Regulated hydropower. The implementation of regulated hydropower aims at finding the balance between modelling the flexibility of hydropower and also including the limits of this flexibility enforced by regulations. Inspired by the modelling in EMPIRE [34], we model the accumulated net water usage with the variable $h_{nt}^{\text{acc,use}}$ and add the possibility to spill water from the reservoir without producing energy. In the following, we let n be some hydro storage node, $\hat{p}$ the stored resource, and the constraints hold for all operational periods $t \in \mathcal{T}$.

In each strategic period, the total water use is limited by H_{nt}^{Budget} (1).

$$-H_{nt}^{\text{Budget}} \leqslant h_{nt}^{\text{acc,use}} \leqslant H_{nt}^{\text{Budget}} \tag{1}$$

When modelling hydro storage without pumping installed, the lower limit in (1) is set to 0. The amount of water used in the production of energy $s_{nt}^{\text{rate,use}}$ is bounded by the installed production capacity $s_{nt}^{\text{rate,inst}}$ (2).

$$s_{nt}^{\text{rate,use}} \leqslant s_{nt}^{\text{rate,inst}} \tag{2}$$

The actual energy output $f_{nt\hat{p}}^{\text{out}}$ of a reservoir n depends on the production efficiency $P_{n\hat{p}}^{\text{out}}$ and the amount of water or energy used $s_{nt}^{\text{rate,use}}$ (3).

$$f_{nt\hat{p}}^{\text{out}} = s_{nt}^{\text{rate,use}} P_{n\hat{p}}^{\text{out}} \tag{3}$$

When modelling a hydro storage with no pump installed, we additionally require that the inflow of the stored resource $\hat{p}$ is zero (4).

$$f_{nt\hat{p}}^{\text{in}} = 0 \tag{4}$$

The energy balance gives the full definition of the accumulated hydro use $h_{nt}^{\text{acc,use}}$ (5), and the accumulated hydro use is restarted for each operational period (6).

$$h_{nt}^{\text{acc,use}} = s_{nt}^{\text{rate,use}} - P_{n\hat{p}}^{\text{in}} f_{nt\hat{p}}^{\text{in}} + h_{nt}^{\text{spill}} - h_{nt}^{\text{tank}} + h_{n,t-1}^{\text{acc,use}} \tag{5}$$

$$h_{n,t-1}^{\text{acc,use}} = 0 \qquad t \in \mathcal{T}^{start} \tag{6}$$

The variable h_{nt}^{tank} is added as a slack variable, to make sure a feasible solution can be found. The data used is split into representative periods, which make up sub-periods of the strategic periods. At the beginning of each sub-period, the accumulated water use $h_{nt}^{\text{acc,use}}$ is reset to zero.

Finally, the operational expenditure (OPEX) of a unit n is decided by (7).

$$o_{nt^{\text{inv}}}^{\text{var}} = \sum (s_{nt}^{\text{rate,use}} O_{nt}^{\text{var}} + h_{nt}^{\text{tank}} T_{nt}^{\text{cost}}) \Delta t \tag{7}$$

Above, T_{nt}^{cost} is some penalty for the slack variable h_{nt}^{tank}.

Linepacking. Local energy systems are ordered as several connected graphs to represent distinct geographical regions. These sub-networks are connected together with transmission links l. A transmission link can have one or several transmission modes m, where selected energy carriers or resources can be exchanged. Linepacking is implemented as a new transmission mode, supplementing the simple default implementations. The implementation details of the geography package can be found in Appendix B.2. The following description of linepacking in Eq. (9) to Eq. (11) is defined for all transmissions $l \in \mathcal{E}$, operational times $t \in \mathcal{T}$, and transmission modes $m \in \mathcal{M}_l$. Eq. (12) and Eq. (13) takes special considerations to representative periods and are defined over different sets of time as specified before the equations.

[1] Soon available as open-source framework at https://github.com/EnergyModelsX

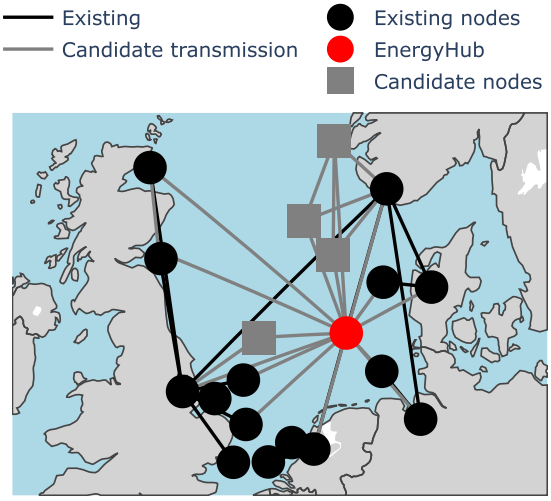

Fig. 1. The model of the energy system in the North Sea with existing and candidate nodes and transmission.

In the current implementation of linepacking, unidirectional flow is required. Thus it is required that the flow of the transmitted resource into the pipeline g^{in}_{ltm} and the amount of flow out g^{out}_{ltm} are both non-negative (8).

$$g^{\text{out}}_{ltm} \geqslant 0, \qquad g^{\text{in}}_{ltm} \geqslant 0 \tag{8}$$

The net volume transmitted into the pipeline is restricted by the transmission capacity g^{cap}_{ltm} (9).

$$g^{\text{in}}_{ltm} \leqslant g^{\text{cap}}_{ltm} \tag{9}$$

A similar constraint holds for the volume transmitted out of the pipeline g^{out}_{ltm} (10).

$$g^{\text{out}}_{ltm} \leqslant g^{\text{cap}}_{ltm} \tag{10}$$

The volume that can be stored in the pipeline due to linepack l^{stored}_{ltm} is bounded by the variable $l^{\text{cap,inst}}_{ltm}$, which again is a ratio of the transmission capacity g^{cap}_{ltm} through the transmission mode parameter $L^{\text{en,share}}_{m}$ (11).

$$l^{\text{stored}}_{ltm} \leqslant l^{\text{cap,inst}}_{ltm} = L^{\text{en,share}}_{m} \cdot g^{\text{cap}}_{ltm} \tag{11}$$

When t is the end of a sub-operational period, the storage level has to be larger or equal to the initial storage level (12).

$$l^{\text{stored}}_{ltm} \geqslant L^{\text{share,init}}_{m} \cdot l^{\text{cap,inst}}_{ltm} \tag{12}$$

The storage in the pipelines are tracked by the energy balance (13). When t is the first time-stage in a sub-operational period $t \in \mathcal{T}^{start}$, the stored level in the pipeline is reset to the product of the initial level ratio $L^{\text{share,init}}_{m}$ and the installed linepack capacity $l^{\text{cap,inst}}_{ltm}$ (14).

$$l^{\text{stored}}_{ltm} = g^{\text{in}}_{ltm} - g^{\text{loss}}_{ltm} - g^{\text{out}}_{ltm} + l^{\text{stored}}_{l,t-1,m} \tag{13}$$

$$l^{\text{stored}}_{l,t-1,m} = L^{\text{share,init}}_{m} \cdot l^{\text{cap,inst}}_{ltm} \qquad t \in \mathcal{T}^{start} \tag{14}$$

3. The north sea case and system description

The model is used in a case study where the main objective is to investigate the potential for offshore electrolysis in the North Sea. The offshore energy system in the North Sea is modelled as shown in Fig. 1, including existing and new HVDC connections, bottom-fixed and floating offshore wind farms based on Durakovic et al. [24]. Offshore electrolysis is an investment option in an offshore energy hub, which is illustrated as a red node in Fig. 1, which can be connected to offshore wind farms and onshore nodes. New HVDC cables can be built on all the line segments in Fig. 1, while H_2 pipelines are investment options between the energy hub and onshore nodes.

3.1. Regions and technologies

The three different types of regions are shown in Fig. 2. In the onshore region, electricity and H_2 markets are modelled by source (supply) and sink (demand) nodes as shown in Fig. 2a. The former is necessary as offshore wind in the North Sea cannot supply all required energy to the neighbouring countries. In addition, H_2 can also be produced from electricity by electrolysis in the onshore region. The net export of H_2 and electricity from the onshore regions is separately limited to 30% of the country's electricity demand to avoid excessive use of the onshore power and H_2 supplies. It is important to note that the onshore nodes can still be used as transit nodes for energy from offshore wind without being affected by the export limit, as offshore wind is defined as separate nodes and sending energy through an onshore node does not add to the net energy export. Hydropower is available in the Norwegian node. In the base case, it is an electricity source that can be regulated while pumped hydropower is included as an option that can be activated based on the case study scenarios.

Existing and potential bottom-fixed offshore wind and potential floating offshore wind power are modelled in the offshore regions as shown in Fig. 2b. Capacity data for the wind farm sites are shown in Table C.1, which is adapted from Durakovic et al. [24]. From the offshore regions, HVDC power transmission is the only investment option. Offshore electrolysis is only available in the energy hub as shown in Fig. 2c, which is connected to other nodes by both H_2 pipelines and HVDC cables.

Technology costs for electrolysis and wind power are shown in Table C.2, while HVDC and pipeline costs are shown in Table C.3. Two different sizes of pipelines are considered; a small pipeline at 4.7 GW and a large pipeline at 13 GW based. The pipelines are based on Jens et al. [35] and have diameters of 900 and 1200 mm respectively. They are modelled as semi-continuous investments such that at least one whole pipeline must be built per investment.

3.2. Temporal resolution and boundary conditions

The model is set up to optimise the development of the joint electricity and H_2 system with four investment periods starting in 2025, 2030, 2040 and 2050. For each of the investment periods, the operation of the system is simulated by 6 representative periods with hourly resolution based on Durakovic et al. [24]. There are 4 weekly periods representing winter, spring, summer and autumn that are used to represent most of the year. In addition, 2 daily periods are included that represent peak energy demand. The peak periods in the EMPIRE model used in [24] are obtained by selecting the two 24 h periods with: (1) the highest demand for a single country and (2) the highest demand for the whole system. This results in a total of 720 operational stages that are scaled to represent the number of operational years within each investment period.

The energy markets in the onshore nodes represent the interactions of the energy system in the North Sea with the rest of the European energy system. The supply side of the energy markets is defined by prices, which are declining towards 2050 for both electricity and H_2. On the demand side, the energy markets are represented by demand profiles, and both electricity and H_2 demand is increasing towards 2050. Onshore nodes are included to represent the energy markets in southern Norway (NOS), Denmark (DK), Germany (GE), the Netherlands (NL) and the United Kingdom (UK). The H_2 demand is emerging from almost nothing in 2025 to significant amounts in 2050 relative to the electricity demand; 30% in the UK and Denmark, 45% in Germany and 80% in The Netherlands. The baseline assumptions for the electricity and H_2 demand and prices are based on the analysis in [24] and shown in Fig. 3. The price range of H_2 of around 155-17 €/MW h in Fig. 3 equals 5.2–0.6 €/kg when converting the H_2 prices to commonly used per mass units by using the LHV of H_2 (33.3 kW h/kg). Similarly, the maximum H_2 demand of 32.7 GW h/h equals 0.98 Mt H_2/h.

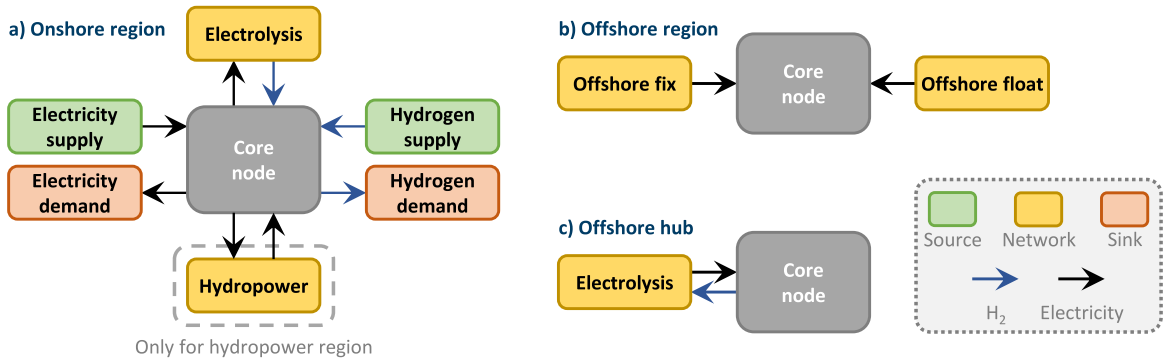

Fig. 2. Three types of regions are defined in the system, (a) onshore regions, (b) offshore regions and (c) offshore hubs.

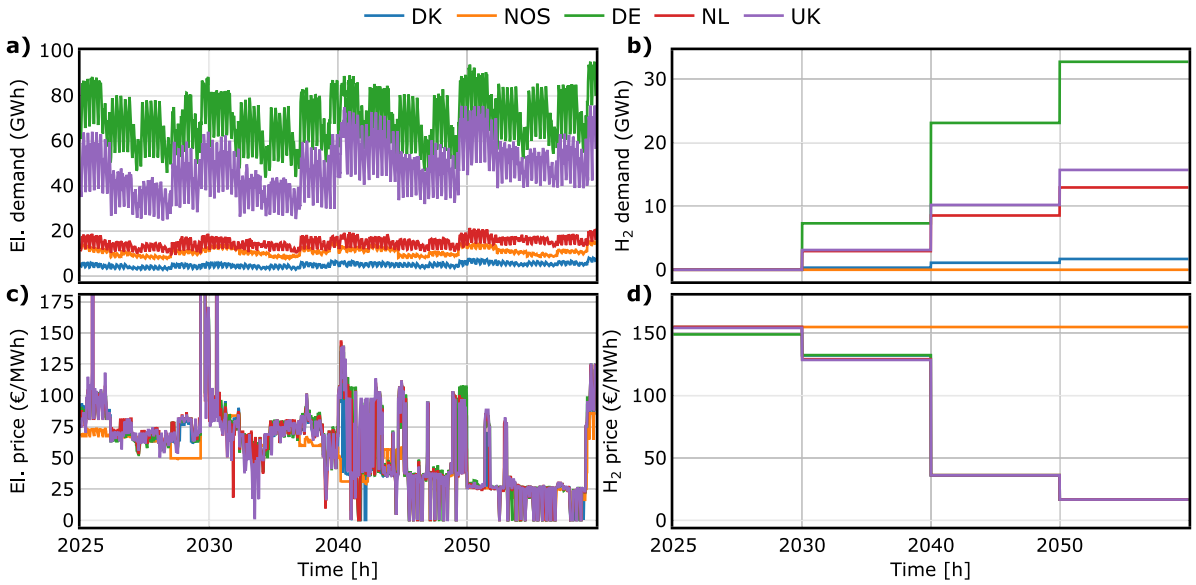

Fig. 3. Sink and source nodes are part of defining boundary conditions. The sink nodes are represented by (a) electricity demand and (b) H_2 demand, while source nodes are represented by (c) electricity prices and (d) H_2 prices. High electricity prices are observed during the peak demand at the end of the first period of upwards of 5000 €/MW h, which is outside of the bounds of the *y*-axis (see supplementary data).

3.3. Case study layout

Offshore electrolysers do not currently exist, thus the CAPEX of this type of electrolysis is highly uncertain. There are several options for technical configuration of offshore electrolysis in the literature either distributed on the turbines, on platforms or on energy islands. Common for all offshore electrolysis is that it requires additional investments that are not strictly necessary for onshore electrolysis, such as sea-water desalination and challenges related to the physical footprint of the equipment [21]. This case study does not consider the technical details of offshore electrolysis, but rather analyses the possible total CAPEX that makes offshore electrolysis attractive compared to onshore electrolysis, assuming the physical operation is similar. The effect of increased CAPEX of offshore installations on the investments in offshore electrolysis is investigated in the first two scenarios by setting the CAPEX to 110% and 120% relative to onshore electrolysis. The sensitivity of the results to different H_2 and electricity prices are investigated by multiplying the baseline of these input parameters, shown in Fig. 3, by a factor of 1–3 and re-running the model. As the baseline H_2 prices do not yield offshore electrolysis, the H_2 price is varied in three levels 2x (low), 2.5x (medium) and 3x (high) the baseline cost assumption. The low H_2 price scenario is only to be considered low in the context of this analysis. The electricity price is varied in four levels: 1x (low), 1.5x (medium), 2x (high) and 2.5x (very high) of the baseline cost assumption.

In the coming analysis, the objective is to analyse other circumstances that can significantly impact the profitability of offshore electrolysis. To this end, three scenarios are studied that build on the case with 120% increased offshore electrolysis CAPEX,

S1 Hydropower with pumping capability.
S2 Tie-in to an existing H_2 pipeline.
S3 Line packing for storing H_2 in pipelines.

In the first scenario S1, the effects of flexible pumped hydropower in Norway are investigated. The second scenario S2 is based on an assumption that, *e.g.*, Europipe II has been repurposed from natural gas to H_2 due to H_2 production in Norway. This scenario allows for a relatively cheap investment in tie-in to the H_2-pipeline, assumed to have a CAPEX of 10% of the investment cost of a similar pipeline on the same distance. We thus want to analyse how large-scale H_2 production in Norway affects investments in offshore electrolysis in the North Sea.

In the third scenario S3, the H_2 pipelines are modelled with the effect of line packing taken into account. This scenario will be used to investigate what effect a more detailed technology representation of the pipeline has on the resulting investments in the North Sea. The estimated line packing capacity of a pipeline is estimated to 0.0129 and 0.0072 MW h/(MW km) for the small and large pipeline respectively based on the equations in Haeseldonckx and D'haeseleer [36] with maximum and minimum pressures of 80 and 40 bar for both pipelines.

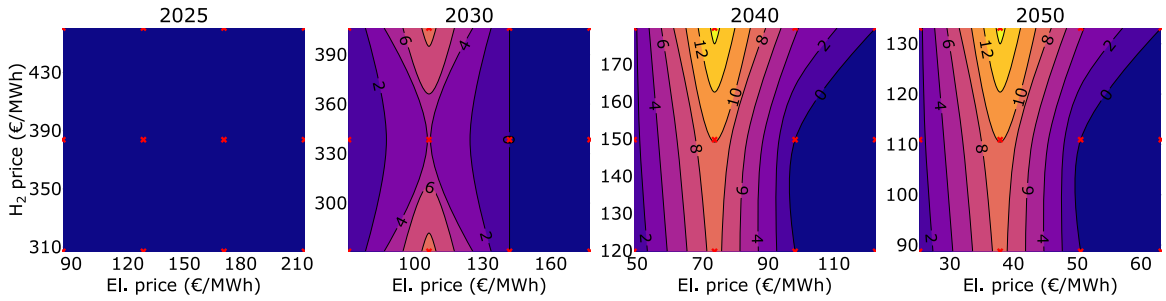

Fig. 4. Sensitivity analyses for 110% offshore electrolysis CAPEX scenario wrt. the H_2 and power prices. The contours show the amount of installed offshore electrolysis (GW), while the red crosses (x) mark the simulated data points.

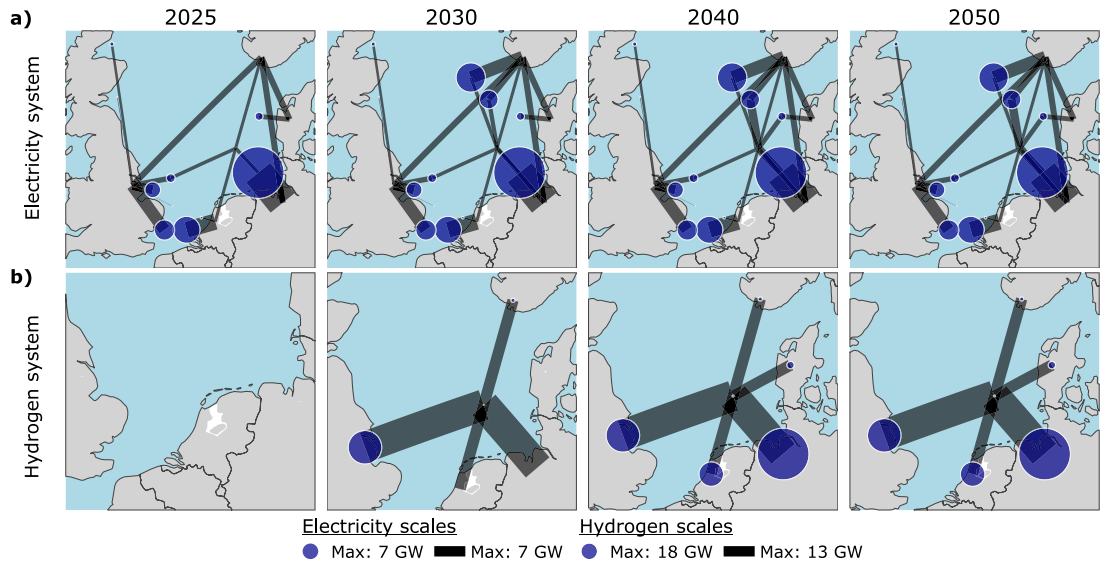

Fig. 5. Energy system for the 110% offshore electrolysis CAPEX scenario with the low H_2 price and low electricity price. (a) Installed capacities of offshore wind and HVDC cables. (b) Installed electrolyser and H_2 pipeline capacity.

The linepacking capacity depends on the flow through the pipeline. This nonlinear effect is not considered in our modelling, instead we use the linepacking capacity at 50% pipeline utilisation. Our numbers for the small pipeline numbers are similar to the numbers in Haeseldonckx and D'haeseleer [37], where a pipeline with a diameter of 900 mm, over 1000 km, operating between 100-40 bar is stated to have a linepacking capability of 65 GW h, equal to 0.0138 MW h/(MW km).

4. Results

4.1. Offshore electrolysis CAPEX of 110%

In the first scenario, the CAPEX of offshore electrolysis is 110% of the onshore electrolysis CAPEX. The results of the sensitivity analysis on prices are shown in Fig. 4, where the x-axis starts at the electricity price baseline and the y-axis starts at 2x the H_2 price baseline. The results in Fig. 4 show that offshore H_2 production at scale requires a higher electricity price than the base assumption, as offshore electrolysis mainly occurs for the medium onshore electricity price (1.5x baseline). On the other hand, a high electricity price reduces the amount of electrolysis offshore as the energy would be more valuable as electricity. At the most beneficial electricity price, the H_2 price has a smaller impact on the installed offshore electrolysis capacity where the installed capacity from 2040 is 8.8, 10 and 14.7 GW for low, medium and high H_2 prices respectively. An interesting observation is that offshore electrolysis develops earlier, already in 2030, for the lowest compared to the medium H_2 price.

The installed capacities in electricity and H_2 infrastructure are shown in Fig. 5(a) and (b) for a low H_2 and low electricity price (lower left datapoint in Fig. 4). Under these assumptions, only 0.2 GW offshore electrolysis is built in 2030, later increasing to 0.7 GW from 2040. The increase is too small compared to the onshore electrolysis to be observable in Fig. 5(b). The installed capacities for HVDC cables and offshore wind farms are shown in Fig. 5(a) for each investment period. In the first investment period, the HVDC link between the UK and Germany is constructed via the offshore hub. Further developments in the electricity system from 2030 include the construction of Sørlige NordsjøI and II wind power plants with capacities of 4.1 and 2.6 GW, where both wind power plants are connected to mainland Norway and the offshore hub. The transmission capacity from Sørlige NordsjøI and II to Norway is 3 and 1.5 GW, while the transmission capacity to the offshore hub is smaller at 0.8 and 0.9 GW respectively. From 2040 the transmission capacity from Sørlige NordsjøII to the offshore hub is expanded to 1.9 GW, while a new transmission line of 1.1 GW is built from the Nordsøen wind power plant, located in Danish waters, to the offshore energy hub.

The development of pipeline and electrolysis capacity in the H_2 system is shown in Fig. 5(b). The offshore hub is mainly used as a transit node for transmitting H_2 from the UK and Norway to Germany and the Netherlands. From 2030, a large H_2 pipeline of 13 GW is built from the UK where 11.7 GW of electrolysis is installed, while a small H_2 pipeline of 4.7 GW is built from Norway where the electrolysis capacity is 1.5 GW. From 2040, significant onshore electrolysis of 8.5 and 18 GW is developed in the Netherlands and Germany respectively. In 2040,

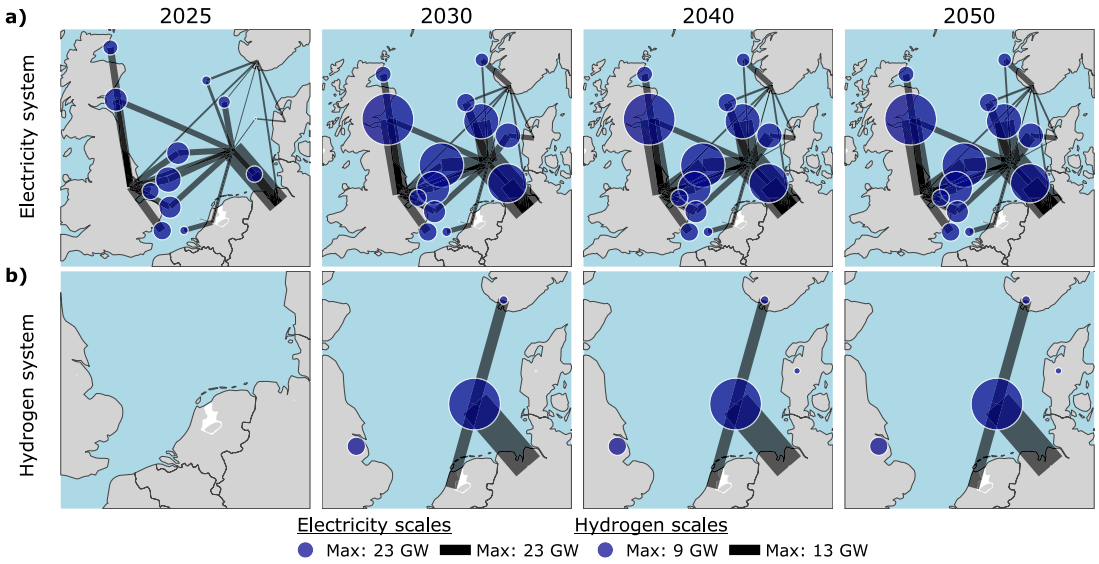

Fig. 6. Energy system for the 110% offshore electrolysis CAPEX scenario with the low H_2 price and medium electricity price. (a) Installed capacities of offshore wind and HVDC cables. (b) Installed electrolyser and H_2 pipeline capacity.

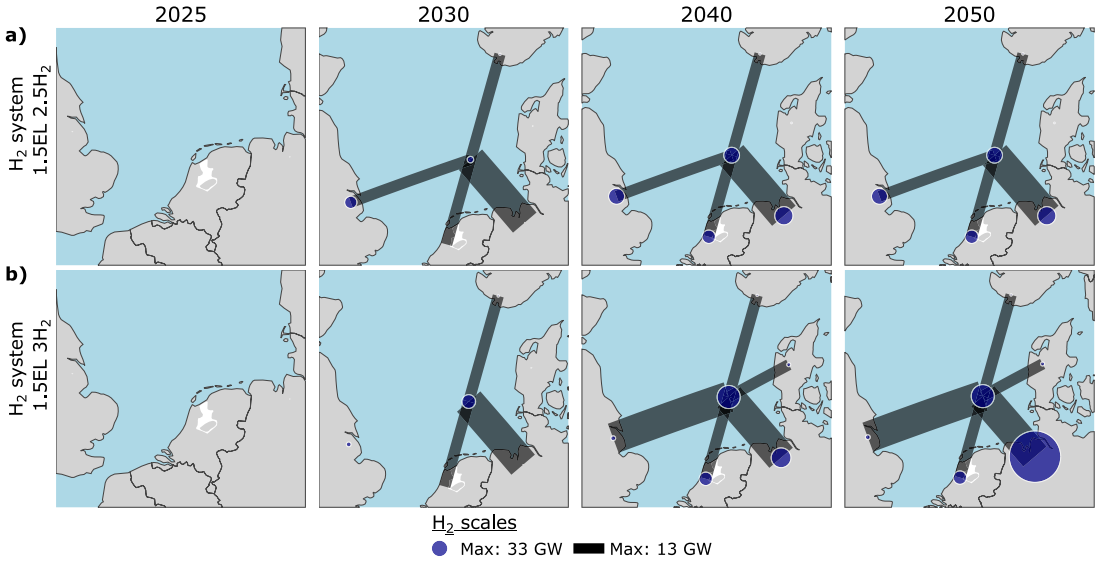

Fig. 7. Installed electrolyser and H_2 pipeline capacity for the 110% offshore electrolysis CAPEX scenario with the medium electricity price and of (a) medium and (b) high H_2 prices.

Denmark is also exporting to the offshore hub through a small pipeline, increasing the electrolysis capacity from 0.3 to 2.6 GW.

Increasing the electricity price to the medium level (1.5x baseline) while keeping the H_2 price low results in significantly more offshore wind power, as shown in Fig. 6, where the total installed capacity in offshore wind increases from 26 GW to 153 GW. Relative to the offshore wind power potential in Table C.1, this represents an increase from 12% to 69%. Installed electrolysis capacity offshore is also significantly higher at 8.8 GW compared to 0.7 GW for the baseline electricity price. The H_2 produced offshore is transmitted to Germany through a large pipeline or to the Netherlands through a small pipeline. The electrolysis capacity and pipeline capacity from Norway remains the same as for the previous case with the lower electricity price. The electrolysis capacity in the UK and Denmark is reduced from 11.7 to 3.1 GW (from 2030) and 2.6 to 1.1 GW (from 2040) respectively, as there are no longer any H_2 exports. Investment in onshore electrolysis in Germany is not profitable in 2030 because onshore electricity is too expensive and the onshore H_2 supply will provide most of the H_2 in 2040 and 2050 for the low H_2 price.

Increasing the H_2 price to medium and high while keeping the electricity price at medium, results in the H_2 system shown in Fig. 7(a) and (b) respectively. The installed capacity in onshore electrolysis and pipelines increases significantly due to the higher H_2 price. For the medium H_2 price, 4.1 GW of offshore electrolysis is installed in 2030 expanding to 10 GW in 2040. In the UK in 2030, 7.8 GW electrolysis are built together with a small H_2 pipeline to the offshore hub. From 2040 onwards, there is a massive increase in onshore electrolysis to 10.2, 8.5 and 11.6 GW in the UK, the Netherlands and Germany respectively. For the high H_2 price, offshore electrolysis is back at the level it was for the low H_2 price of 8.8 GW in 2030 and increases further to 14.7 GW from 2040. The UK is no longer exporting H_2, it is rather imported from the energy hub through a large H_2 pipeline from 2040, while local onshore electrolysis is reduced to 3.1 GW, which is the same as for the low H_2 price. Increased onshore electrolysis is found in Denmark where it increases from 1.1 GW for the medium H_2 price to 2.6 GW and a small

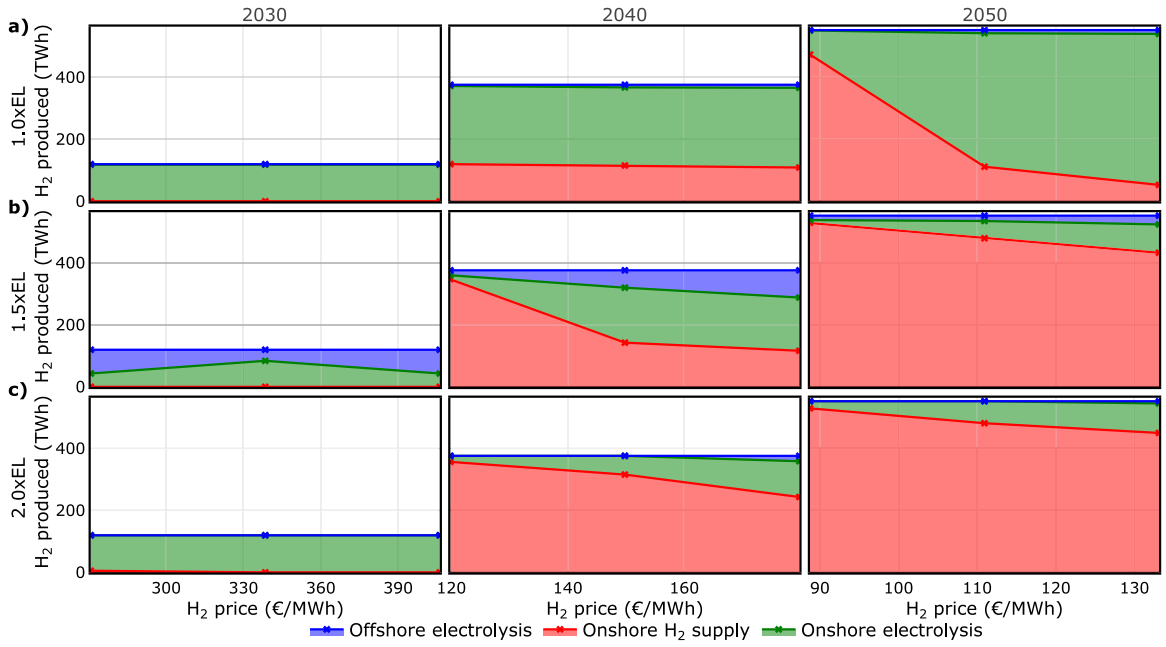

Fig. 8. H_2 produced from offshore electrolysis, onshore electrolysis and bought from the onshore H_2 supply as a function of the H_2 price in the 110% offshore electrolysis CAPEX scenario. Each row corresponds to (a) low, (b) medium and (c) high electricity price levels.

H_2 pipeline for exports to the energy hub. Germany becomes more self-supplied with H_2 produced through onshore electrolysis with a capacity of 8.6 GW in 2040 and 32.7 GW from 2050.

The source of the produced H_2 is plotted as a function of the H_2 price and for the low, medium and high electricity prices in Fig. 8. Onshore electrolysis is dominating in 2030 for baseline electricity prices as shown in Fig. 8(a). About 1/3 of the H_2 is provided by the onshore supply in 2040, while the rest is supplied from onshore electrolysis, and the shares are not sensitive to the H_2 price. On the other hand, the H_2 source is very sensitive to the H_2 price in 2050 where the onshore H_2 supply is providing 86% of the H_2 at a price of 90 €/MW h, while it almost switches completely at 110 €/MW h to 78% from onshore electrolysis. Increasing the electricity price to the medium level as shown in Fig. 8(b) significantly increases H_2 produced from offshore electrolysis. In 2030, H_2 is produced either from onshore or offshore electrolysis where the share of H_2 from each source is dependent on the H_2 price. For low and high H_2 prices 65% is produced offshore, while for the medium electricity price 70% is produced onshore due to the exports from the UK as discussed. In 2040, the onshore H_2 supply is more competitive and the dominating H_2 source for the lower H_2 price, while the medium H_2 price favours both onshore (47%) and offshore electrolysis (15%) and the high H_2 price favours offshore electrolysis, which increase to 23%. The H_2 produced from onshore and offshore electrolysis for the medium to high H_2 price is reduced by 54–69% from 234–260 TW h to 73–120 TW h from 2040 to 2050, while capacities mostly remains the same and are even increased in Germany for the highest H_2 price as shown in Fig. 7(b). In 2050, the system favours buying more H_2 from the onshore supply as the prices are generally low even for the highest H_2 prices. H_2 from electrolysis is only profitable in hours with very low electricity prices, which is assumed to be common in 2050 as shown in Fig. 3(c). Electrolysis is again dominating in 2030 for the highest electricity price in Fig. 8(c), while the onshore H_2 supply takes over in 2040 and 2050. The onshore H_2 deliver 65% of the total H_2 demand in 2040 and 81% in 2050 for the highest H_2 supply price, supplemented by a smaller share of H_2 mostly from onshore electrolysis which is increasing with the H_2 price up to 31% in 2040 and 17% in 2050.

4.2. Offshore electrolysis CAPEX of 120%

Increasing the CAPEX of offshore electrolysis to 120% of onshore electrolysis makes it significantly less attractive as shown in Fig. 9. There is no longer any offshore electrolysis for the low H_2 price. While there are no longer any investments in offshore electrolysis in 2030, keeping the electricity price at the medium level and increasing the H_2 price to medium and high results in the most installed capacity in offshore electrolysis of 2.3 and 5.7 GW from 2040. Thus, the installed capacity for offshore electrolysis is almost reduced to a third from the 110% scenario in Section 4.1, which is a reduction from 14.7 GW to 5.7 GW in the most extreme case. In the case of the low electricity prices and medium to high H_2 prices, investments in offshore electrolysis in 2040 are lower at 0.7 and 1.1 GW respectively.

The development of the H_2 system is shown in Fig. 10 for a medium electricity price and (a) low, (b) medium and (c) high H_2 prices. In 2030, the H_2 system is the same for all electricity prices. Onshore electrolysis of 11.9 GW is built in the UK, 1.5 GW in Norway and 0.3 GW in Denmark. A large H_2 pipeline is built from the UK and a small H_2 pipeline from Norway to the energy hub, a large and a small H_2 pipeline is built from the energy hub to Germany and the Netherlands respectively. For 2040 and 2050, the investments in the H_2 system differ depending on the price of H_2 supply. For the low H_2 price in Fig. 10(a), there are only small investments from 2040, where onshore electrolysis in Denmark increase to 1.1 GW. Increasing the H_2 price to the medium price level results in 2.3 GW offshore electrolysis and 8.5 and 17.7 GW onshore electrolysis in the Netherlands and Germany as shown Fig. 10(b), while there are no changes to electrolysis in the UK, Norway and Denmark or H_2 pipelines compared to the low H_2 price case. For the highest H_2 price in 2040, 5.7 GW of offshore electrolysis is installed and a small H_2 pipeline is built to the energy hub from Denmark where 2.6 GW of electrolysis is installed. The investment in onshore electrolysis in Germany is delayed for the high H_2 price compared to the medium H_2 price, where 12.8 GW is installed 2040 and increasing to a total of 29 GW in 2050. An offshore cost premium of 130% was also tested, which resulted in no offshore electrolysis.

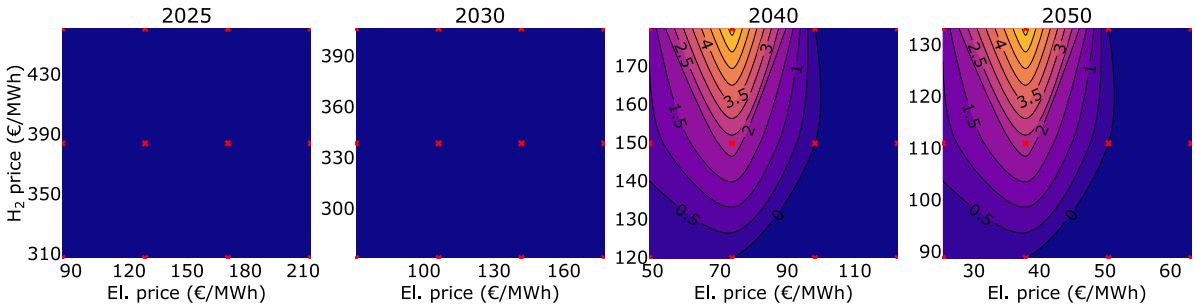

Fig. 9. Sensitivity analyses for 120% offshore electrolysis CAPEX scenario wrt. the H_2 and power prices. The contours show the amount of installed offshore electrolysis (GW), while the red crosses (x) mark the simulated data points.

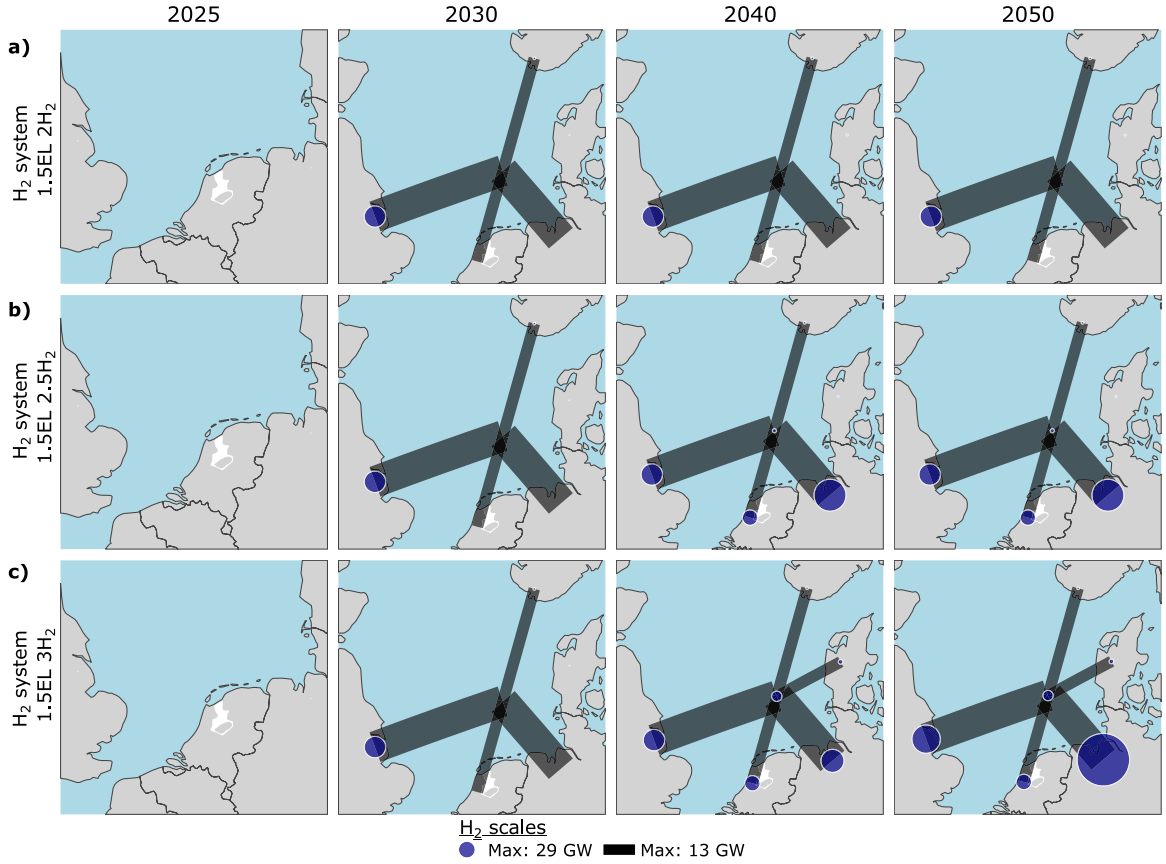

Fig. 10. Installed electrolyser and H_2 pipeline capacity for the 120% offshore electrolysis CAPEX scenario with medium electricity price and (a) low, (b) medium and (c) high H_2 prices.

4.3. Infrastructure scenarios

The offshore electrolysis CAPEX is kept at 120% of onshore electrolysis. Three scenarios investigate different technical solutions that impact the investment or operational costs in the case study; H_2 tie-in to Europipe 2 at the energy hub, pumped hydropower in Norway and energy storage in pipelines through H_2 linepacking. The 120% scenario in Section 4.2 is used as a reference for the infrastructure scenarios.

In the tie-in scenario, the model has the option to invest in a tie-in to an existing pipeline that is passing close to the offshore hub on the way to Germany. The CAPEX is assumed to be 10% of a normal pipeline and the pipeline has a capacity of 14.5 GW. For the tie-in scenario, there was no noticeable difference in the invested capacities compared to the 120% reference scenario other than an increased pipeline capacity from the offshore hub to Germany from 13 to 14.5 GW. This is because the cost of the pipeline is small compared to other costs, thus this scenario is not discussed further.

4.3.1. Pumped hydropower in Norway

In order to estimate the maximum impact pumped hydropower can have on offshore electrolysis in the North Sea, all the hydropower plants in southern Norway are given the ability to consume power and pump water back into the reservoirs. This has a much more significant effect compared to the tie-in, as shown in Fig. 11. For the low electricity price, the installed capacity in offshore electrolysis in 2040 increases with 0.5–0.6 GW from the reference case in Section 4.2. The effect of pumped hydropower on offshore electrolysis is larger when the electricity price is increased, where the medium and high electricity prices result in 1–1.3 GW and 1.6 GW more installed offshore electrolysis capacity respectively. The highest installed offshore electrolysis is 7 GW for the medium electricity price and high H_2 price. The installed H_2 pipeline capacities are identical to the results from the reference scenario without pumped hydropower as shown in Fig. 10. For the installed onshore electrolysis capacity, the increase in offshore electrolysis is compensated by reducing the onshore electrolysis by the

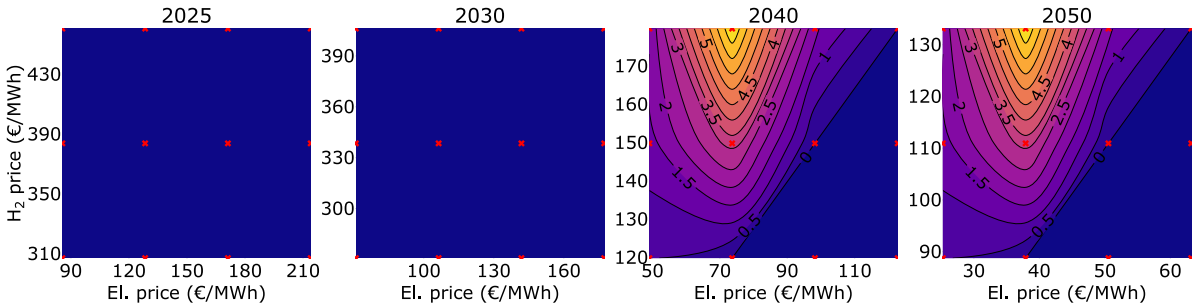

Fig. 11. Sensitivity analyses for the case with 120% offshore electrolysis CAPEX and pumped hydropower in Norway wrt. the H_2 and power prices. The contours show the amount of installed offshore electrolysis (GW), and the red crosses (x) mark the simulated data points.

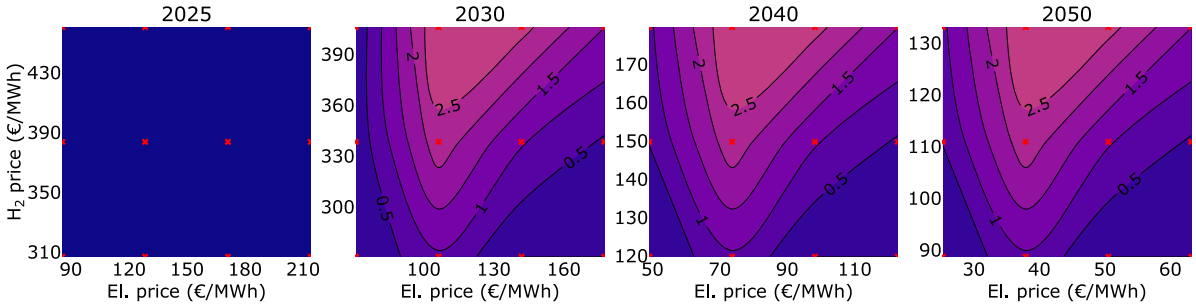

Fig. 12. Sensitivity analyses for the case with 120% offshore electrolysis CAPEX and H_2 linepacking wrt. the H_2 and power prices. The contours show the amount of installed offshore electrolysis (GW) and the red crosses (x) mark the simulated data points. Note that the very high electricity price is not included.

same amount, mostly in Germany, but there is also a small reduction of electrolysis in Norway.

4.3.2. Linepacking

Linepacking results in earlier adoption of offshore electrolysis where all the capacity is installed in 2030, as shown in Fig. 12. Installed capacities in offshore electrolysis are more robust against variations in electricity and H_2 prices, while the peak installed capacity at 3 GW is lower than in the base and pumped hydropower case of 5.7 and 7 GW, respectively. Low H_2 and high electricity prices have less of a negative impact on the installed offshore electrolysis compared to the other cases. For the highest electricity price and the medium and high H_2 prices, the installed offshore electrolysis is 0.4 and 1.5 GW respectively, while no offshore electrolysis is found for those prices in the other cases. The linepacking introduce 0.9 GW of offshore electrolysis for the medium electricity price and low H_2 price, where H_2 prices previously where too low for offshore electrolysis to be profitable. The positive effects on offshore electrolysis capacity at high electricity prices and low H_2 prices can be attributed to H_2 production from surplus energy that can be stored in the pipelines resulting in less energy curtailment.

The H_2 system capacities are plotted for the linepacking scenario with the medium electricity price in Fig. 13, where the low, medium and high H_2 price cases are shown in (a), (b) and (c), respectively. All investments in the H_2 system occur in 2030 for the low H_2 price, where large H_2 pipelines are built from the UK to the energy hub. From the energy hub a small H_2 pipeline is built to the Netherlands and a large H_2 pipeline to Germany. The electrolysis capacity in the UK is 15.5 GW, which is an increase of 30% from the reference scenario. Offshore electrolysis increases from nothing in the reference scenario to 0.9 GW. There is no longer any electrolysis or H_2 export from Norway, which in the reference case had 1.5 GW of electrolysis capacity.

There is a significant difference in H_2 infrastructure investments from the low to the medium H_2 price with a more extensive H_2 pipeline network connecting all of the countries in the case study. In 2025, a small H_2 pipeline is built from Norway to the offshore energy hub as shown in Fig. 13(b) even though the electrolysis capacity in Norway is only 11.4 MW, while a large H_2 pipeline connects the energy hub to Germany. From 2030 the UK is connected to the energy hub through two 14.2 GW H_2 pipelines, one in each direction. Two large H_2 pipelines are built from the energy hub to the Netherlands and Germany, while a small H_2 pipeline is built to Denmark. The electrolysis capacity is significantly increased with new capacity of 15.5 GW in the UK and 2.3 GW at the energy hub and a total of 1.5 GW of electrolysis in Norway. More electrolysis capacity is added in 2040, 8.5 GW in Netherlands, 40.2 GW in Germany and 1.1 GW in Denmark. A new pipeline of 17.1 GW is built from Germany to the energy hub. No new investments are made in H_2 infrastructure in 2050 for the medium H_2 price.

For the high H_2 price in 2025 and 2030, the H_2 infrastructure is similar to the medium H_2 price. The difference is that offshore electrolysis is increased to from 2.3 to 3 GW in 2030 and pipeline capacity is reduced from 14.2 to 13 GW between the offshore hub and the UK. The changes are more apparent in 2040 and 2050 with large increases of electrolysis, especially in Germany as shown in Fig. 13(c). The electrolysis capacity in Germany increases to 43.8 and 54.7 GW, accompanied with a pipeline to the energy hub of 56.4 GW and a pipeline from the energy hub to Germany of 64.6 GW. There is also an increase in the electrolysis capacity in the UK from 15.5 GW in 2030 to 20.7 GW in 2040. The total installed electrolysis capacity when linepacking is included is significantly higher than for the base and pumped hydro case. For medium electricity and H_2 prices, the total electrolysis capacity in 2040 increases from 43 to 69.1 GW as a result of linepacking. Linepacking makes onshore electrolysis much more competitive to the onshore H_2 supply, which results in a large uptake of energy from the electricity market. This is seen especially in 2040 and 2050, where electricity prices are highly variable with periods of free electricity.

For low electricity prices, the quantities of H_2 produced from onshore electrolysis represent 69–80% and 16–92% of the total H_2 demand in 2040 and 2050 respectively, where the range depends on the H_2 price. This represents an increase in onshore electrolysis from the reference scenario by 13–15% and 3–5% in 2040 and 2050. Increasing the onshore electricity price reduces the quantities of H_2 from onshore electrolysis and increases the use of the onshore H_2 supply. There is

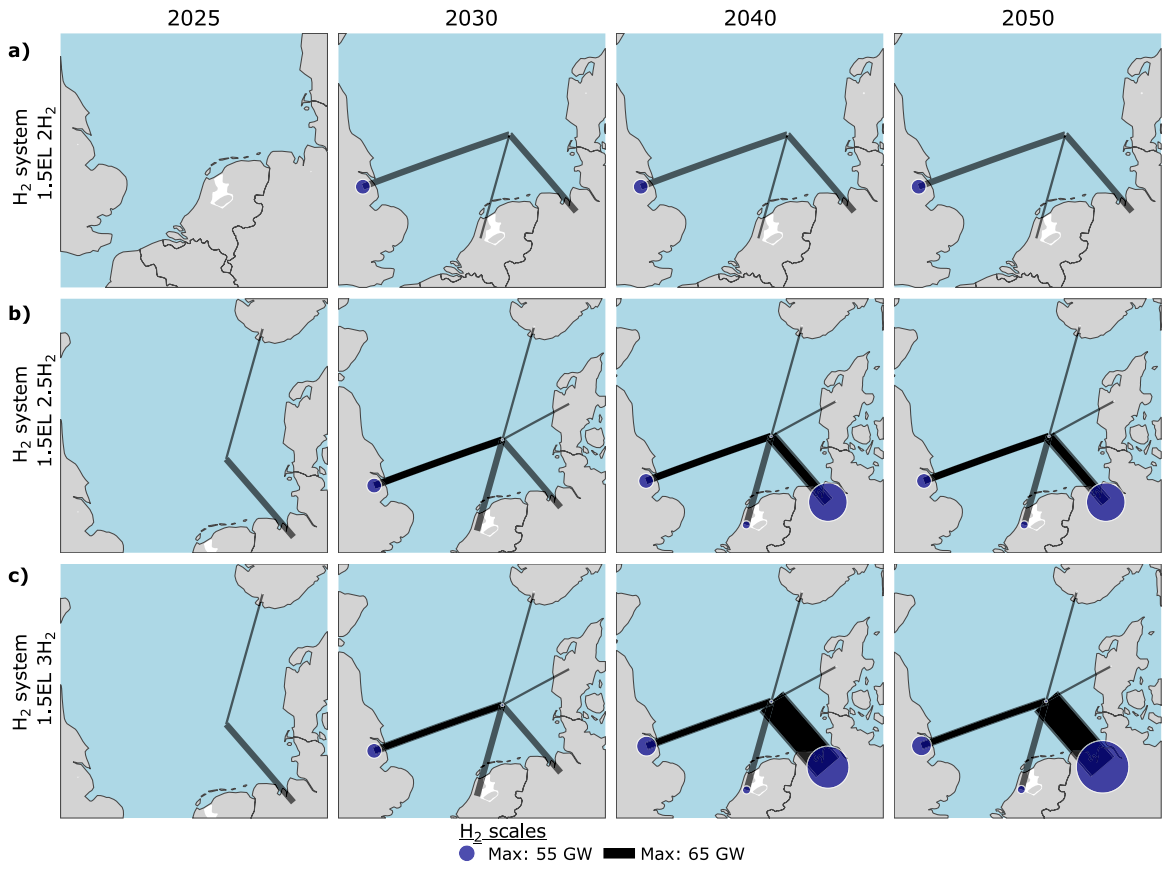

Fig. 13. Installed electrolyser and H_2 pipeline capacity for the linepacking scenario with the medium electricity price and (a) low and (b) medium and (c) high H_2 prices.

almost no onshore electrolysis for the low H_2 price, while medium electricity prices combined with the highest H_2 price result in shares of onshore electrolysis of up to 74% and 29% in 2040 and 2050 respectively, up from 59% and 19% in the reference case. The high electricity and H_2 prices results in 48% and 22% shares of the H_2 from onshore electrolysis in 2040 and 2050 respectively, up from 33% and 19% in the reference case.

5. Discussion

All cases that lead to significant offshore electrolysis require scaling of both the H_2 price and the electricity price from the levels given by the baseline assumptions from Durakovic et al. [24]. While the prices are scaled independently, investments in onshore electrolysis make sure that the H_2 prices and the electricity prices are interdependent. The electricity price is shown to be the most critical parameter and has to be at a suitable level for electrolysis to be competitive offshore. There is a window of opportunity for offshore electrolysis for the two base scenarios with increased offshore electrolysis CAPEX of 110% and 120%. The sensitivity analyses show that a medium electricity price, which is 1.5x the baseline price assumption, gives the highest installed capacities of offshore electrolysis. This window of opportunity is a result of the increased onshore electrification and higher electricity prices that leads to a large build-out of offshore wind resulting in a surplus of electricity offshore. However, if the onshore electricity price is too high, the energy is more valuable as electricity even for high H_2 prices, and will be transported onshore at the expense of extra losses from curtailment. On the other hand, if the electricity price is too low, onshore electricity supply will be used to produce H_2 through onshore electrolysis. Thus low electricity prices are not sufficient to create enough surplus of electricity from offshore wind to make offshore electrolysis profitable. The level of the electricity price partially depends on the availability of alternative methods for electricity production, such as onshore wind and solar power, that are not included directly in this analysis but rather represented by the onshore electricity price.

The results show that the H_2 price has to be at a certain level depending on the premium of offshore installations for offshore electrolysis to be an attractive investment. Increasing the CAPEX of offshore electrolysis from 110% to 120%, reduces the installed capacity by 7.7–9 GW (61–100%) for the medium electricity price cases. Offshore electrolysis is no longer profitable if the CAPEX is increased further to 130%. This highlights that the construction costs for offshore electrolysis cannot be much higher than electrolysis onshore. Otherwise, it would be better to transport the electricity onshore and produce H_2 there. Typically, the costs of building infrastructure offshore is more expensive than onshore. In the case of electrolysis, it would require a desalination plant. There is also a larger focus on spacial requirements offshore that would likely require the usage of proton-exchange membrane (PEM) electrolysis over alkaline electrolysis, which are currently more expensive, but are expected to become cheaper in the coming years.

Offshore electrolysis can have an impact on the import and export from the UK. From the analysis of the 110% offshore electrolysis case, as is shown in Fig. 6(b) and Fig. 7, there is an opportunity for the UK to export H_2 at the medium H_2 price. However, if the H_2 price is too high this switches to import to the UK from the offshore hub. In other words, the H_2 price has to be high enough that it is profitable to build the infrastructure needed to produce and export H_2, but not too high as H_2 from the onshore supply is needed to balance the H_2 production from variable offshore wind power in the UK. The export from the UK reduces the need for offshore electrolysis in 2030 for the medium H_2 price, as shown in Fig. 4, where the offshore electrolysis investments

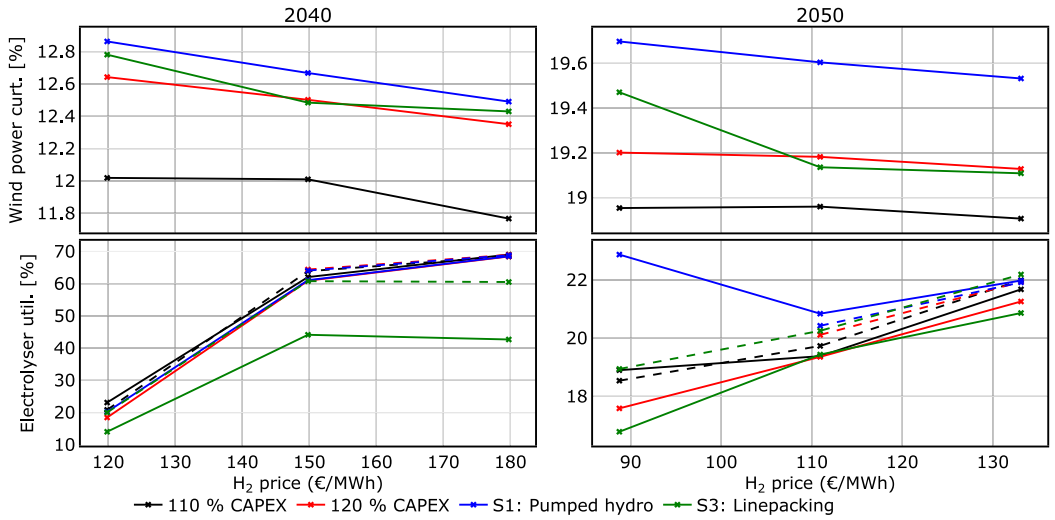

Fig. 14. Wind power curtailment and utilisation of electrolysis capacity comparison between the scenarios for 2040 and 2050. Wind power curtailment and electrolyser utilisation is plotted for the system as a whole wrt. H_2 prices for the medium electricity price. Offshore electrolyser utilisation is shown as a separate dotted line.

are delayed to 2040. On the other hand, imports to the UK are facilitating offshore electrolysis for the high H_2 price. In comparison, Germany which is the largest consumer of H_2, is always importing H_2 and responds to higher H_2 prices by increasing its onshore H_2 electrolyser capacity. In the 120% scenario, the electrolysis capacity in the UK stays constant independent of the H_2 price for the medium electricity price scenario, except an increase of 3.8 GW in 2050 for the highest H_2 price. This indicates that the offshore hub is competitive against the UK for producing H_2 if offshore electrolysis is relatively inexpensive compared to onshore electrolysis. Offshore electrolysis has the advantage that it is located at a hub for electricity transmission close to offshore wind farms which give low electricity prices. Furthermore, the electricity is received from many locations with lower correlation between wind profiles that results in 3–4% higher electrolyser capacity utilisation.

The H_2 export from the Nordic countries, Norway and Denmark, is largely independent of the cost for offshore electrolysis. While H_2 export from Norway is profitable independent of the H_2 price, H_2 export from Denmark requires the highest H_2 price. Norwegian H_2 export is a result of more stable electricity prices in Norway as flexible hydropower can balance new offshore wind power production. A stable electricity price increases the capacity utilisation and cost-effectiveness of the electrolysers, which is 30–40% points higher in Norway compared to the other countries. For medium and high H_2 prices the capacity utilisation of electrolysis in Norway typically close to 100%. The utilisation of electrolyser capacity in Denmark is also higher than the other countries at 70–80%.

The Netherlands and Germany are typically the largest importers of H_2 from the offshore hub as they are large consumers of energy and have relatively low amounts of offshore wind on their shores. If the H_2 price is high, Germany becomes a large producer of H_2 from onshore electrolysis with upwards of 33 GW installed capacity without linepacking and 54.7 GW with linepacking. Large H_2 pipeline capacities are used to transport H_2 to Germany from the offshore hub, especially in the linepack case where 64.6 GW of pipelines are built from the energy hub to Germany and a pipeline of 56.4 GW is built in the opposite direction.

Wind power curtailment and utilisation of the electrolysis capacity from the scenarios with different offshore electrolysis CAPEX and infrastructure scenarios are compared in Fig. 14 for the medium electricity price in 2040 and 2050. The case with higher offshore electrolysis CAPEX results in 0.5–0.6% higher curtailment and slightly lower electrolyser capacity utilisation. Wind power curtailment is only reduced by up to 0.4% with increasing H_2 prices for all the scenarios. The pumped hydropower scenario has a slightly higher level of wind power curtailment compared to the reference scenario of 0.1–0.2% and 0.4–0.5% in 2040 and 2050 respectively. The higher wind power curtailment can be related to the periods of low and sometimes zero electricity prices from the onshore electricity supply that can be utilised to pump water back into the reservoirs. In this case, it is better to build less HVDC cables to the Norwegian offshore wind power farms and waste more wind power resources, which increases the utilisation of the HVDC capacity. In general, the curtailment is high at 12–13% and 19%–20% in 2040 and 2050, which illustrate the challenges with introducing large amounts of offshore wind into the electricity system.

The electrolysis utilisation is increasing with higher H_2 prices for all scenarios as more hours have sufficiently low electricity prices that also lead to more stable H_2 production. Similarly, we observe the opposite effect when varying the electricity prices. A low electricity price leads to higher utilisation at 70%, also for low H_2 prices, and higher electricity prices lead to low utilisation, also for high H_2 prices. The low capacity utilisation seen in 2050 is a result of very low H_2 prices at 0.6 €/kg, which only makes it profitable to produce H_2 through electrolysis in periods with extremely low electricity prices. Producing electrolytic H_2 in low-price periods will in turn help to increase the electricity price and make it more stable, but to which extent is dependent on the H_2 price and demand. Storing H_2 by linepacking makes it possible to produce more H_2 in low price periods, which results in even lower capacity utilisation as shown in Fig. 14. It is better to run the onshore electrolysis with low capacity utilisation due to the lower CAPEX compared to offshore electrolysis, thus the onshore electrolysis capacity utilisation is 16–17% and 1–2% points lower in 2040 and 2050 respectively for the medium and high H_2 prices.

An aspect that could be further improved is the modelling of boundary conditions represented by the onshore electricity and H_2 supplies. Limiting the available energy exchange between countries is a simplified approach that can give more realistic results than unlimited supplies. An improved, future approach, could be to include price-sensitive supplies and demands. The amount of electrolysis installed and running with low utilisation factors is likely overestimated as the demands are not price-sensitive (elastic) in the conducted case study. Another reason to limit the net energy transferred between the onshore supplies is that some cross-border energy supply is already included in the supply prices as they are obtained from the dual value of the energy balance from Durakovic et al. [24]. Finally, as the share of offshore wind increases, it will eventually be the dominating energy supply from the North Sea region and the utilisation of local transmission capacities.

A second improvement is allowing energy transfer between the individual countries that does not have to be routed via the energy hub.

This might also impact the amount of offshore electrolysis. Allowing the H_2 pipelines to use linepacking showed to have a significant effect on the results. We emphasise that these results provide an estimate to the potential of H_2 linepacking in an energy-system perspective, while the technical ability of pipelines to pack H_2 is uncertain as it is not currently utilised at scale. The real linepacking ability of a H_2 pipeline depends on several parameters such as the maximum and minimum pressure, length, number of compressor stations as well as the flow through the pipeline [36]. A more detailed modelling of pipelines that includes the impact of the gas flow and other parameters on the linepacking capacity is needed to get a better understanding of the potential of H_2 linepacking and the impact of this operational strategy on the energy system [30]. Furthermore, competitive ways of utilising the flexibility that H_2 offers should be considered such as storage in salt caverns or other forms of storage and using H_2-fuelled gas turbines, which might reduce the usage of linepacking.

6. Conclusion

When analysing the conditions necessary for offshore electrolysis in the North Sea, we find that for an offshore electrolysis capacity cost of 110% of onshore electrolysis, the onshore electricity price has to be 150% of the baseline to get significant amounts of offshore electrolysis of 8.8, 10 and 14.7 GW for low, medium and high H_2 prices. Lower electricity prices do not lead to sufficient electricity available from offshore wind to make offshore electrolysis attractive. Higher electricity prices lead to less offshore electrolysis as the electricity is more valuable than H_2 at the cost of increased curtailment. The same window-of-opportunity with respect to the electricity and H_2 prices is observed for a 120% offshore electricity CAPEX compared to onshore electrolysis, but with offshore electrolysis capacity reduced to around a third of the capacity at around 5.7 GW for the most beneficial case. A 130% offshore CAPEX cost premium yields no offshore electrolysis.

The case studies show that the UK can be an exporter of H_2 due to the large offshore wind resources. However, this depends on the cost premium of offshore electrolysis and the H_2 price, where offshore electrolysis can compete with UK electrolysis if the offshore electrolysis cost premium is low. On contrary, Germany and the Netherlands will import large amounts, unless the onshore H_2 prices are 2.5x the baseline or higher. Norway exports H_2 to the offshore hub as it has suitably low electricity prices and superior utilisation of the electrolysis capacity close to 100% compared to other countries because of hydropower flexibility. Denmark will also export H_2 if the H_2 price is higher than 3x the baseline in the 110% CAPEX case, as the utilisation of electrolyser capacity is relatively high, typically around 70–80%, compared to the other countries.

With the 120% offshore electrolysis CAPEX scenario as a basis, three infrastructure scenarios are tested with (1) tie-in to existing H_2 pipelines from the energy hub to Germany, (2) pumped hydropower in Norway and (3) linepacking of H_2 in pipelines. A tie-in showed to have little effect on the H_2 infrastructure investments because the cost for new pipeline capacity is low compared to other costs in the system. Even though the pipeline costs in itself is rather expensive. Pumped hydropower results in a maximum installed offshore electrolysis capacity of 7 GW, which is an increase of 1.6 GW from the reference case. Pumped hydropower also led to slightly higher wind power curtailment and electrolysis capacity utilisation.

Linepacking of H_2 pipelines makes offshore electrolysis more robust to low H_2 prices and high electricity prices. The maximum installed offshore electrolysis capacity is lower for the linepacking case, while installed onshore electrolysis capacity increases significantly. Linepacking results in a large increase of electrolysis capacity in Germany from a maximum of 29 GW without to 54.7 GW with linepacking. The same effect is shown on the H_2 pipeline investments that increase from 13 GW without to 64.6 GW with linepacking. The capacity utilisation of onshore electrolysis is lower when linepacking is included, while the capacity utilisation for offshore electrolysis remains higher due to the higher CAPEX. The wind power curtailment show low sensitivity to increasing H_2 prices and decreases with less than 0.4% points from the low to the high H_2 price.

CRediT authorship contribution statement

Espen Flo Bødal: Writing – review & editing, Writing – original draft, Visualization, Validation, Software, Methodology, Investigation, Formal analysis, Data curation, Conceptualization. **Sigmund Eggen Holm:** Writing – review & editing, Writing – original draft, Software, Methodology, Investigation, Conceptualization. **Avinash Subramanian:** Software, Methodology, Investigation, Conceptualization. **Goran Durakovic:** Writing – review & editing, Validation, Resources, Investigation, Data curation, Conceptualization. **Dimitri Pinel:** Writing – review & editing, Software, Methodology, Conceptualization. **Lars Hellemo:** Writing – review & editing, Software, Methodology, Conceptualization. **Miguel Muñoz Ortiz:** Writing – review & editing, Software, Methodology, Conceptualization. **Brage Rugstad Knudsen:** Writing – review & editing, Writing – original draft, Software, Project administration, Methodology, Investigation, Funding acquisition, Conceptualization. **Julian Straus:** Writing – review & editing, Writing – original draft, Visualization, Software, Project administration, Methodology, Investigation, Funding acquisition, Formal analysis, Conceptualization.

Declaration of competing interest

The authors declare the following financial interests/personal relationships which may be considered as potential competing interests: All authors reports financial support was provided by Research Council of Norway.

Data availability

Data for: "Hydrogen for harvesting the potential of offshore wind: A North Sea case study" (Original data) (Zenodo)

.

Acknowledgements

This publication has been funded by the CleanExport project - Planning Clean Energy Export from Norway to Europe, 308811. The authors gratefully acknowledge the financial support from the Research Council of Norway and the user partners Å Energi, Air Liquide, Equinor Energy, Gassco and TotalEnergies OneTech. The authors gratefully acknowledge Gurobi for providing a licence for solving the optimisation problem.

Appendix A. Nomenclature

Indices	
a	Area
l	Link or transmission
m	Transmission mode
n	Node
p	Resource
t	Operational period
t^{inv}	Investment period
Parameters	
Δt	Length of operational period

$C^{\text{max,add}}_{nt^{\text{inv}}}$	Maximum allowed added capacity
$C^{\text{max,inst}}_{nt^{\text{inv}}}$	Max installed capacity
$C^{\text{min,add}}_{nt^{\text{inv}}}$	Minimum allowed added capacity
C^{Init}_{nt}	Initial capacity
$C^{\text{trans,max,add}}_{lmt^{\text{inv}}}$	Maximum allowed added transmission capacity
$C^{\text{trans,max,inst}}_{lmt^{\text{inv}}}$	Max installed transmission capacity
$C^{\text{trans,min,add}}_{lmt^{\text{inv}}}$	Minimum allowed added transmission capacity
D^{deficit}_{nt}	Penalty for deficit at sink
D^{surplus}_{nt}	Penalty for surplus at sink
E^{Int}_{p}	Emission intensity of resource
$E^{\text{cost}}_{pt^{\text{inv}}}$	Cost per unit of emitted product
E_{np}	Emissions rate per produced unit
H^{Budget}_{nt}	The budgeted water use for a hydro storage
L^{min}_{nt}	Minimum allowed reservoir level, as a ratio of $s^{\text{cap,inst}}_{nt}$
$L^{\text{share,init}}_{m}$	Linepack initial storage, ratio of capacity
$L^{\text{en,share}}_{m}$	Linepack storage capacity of a pipeline
$O^{\text{fix}}_{nt^{\text{inv}}}$	Fixed operational cost
O^{var}_{nt}	Variable operational cost
P^{in}_{np}	Input of resource per produced unit
P^{out}_{np}	Output of resource per produced unit
R^{Capture}_{n}	CO_2 capture rate
R^{Inflow}_{nt}	Inflow into a reservoir
R^{Init}_{nt}	Initial reservoir level
T^{cost}_{nt}	Penalty for hydro storage slack variable
$T^{\text{cap,init}}_{m}$	Installed capacity of transmission mode
T^{loss}_{m}	Rate of loss for a transport mode
W^{profile}_{nt}	Profile for a renewable source, a time series of ratios
$X^{\text{capex,cap}}_{nt^{\text{inv}}}$	CAPEX cost per capacity unit
$X^{\text{capex,trans}}_{lmt^{\text{inv}}}$	CAPEX cost per capacity unit

Sets

$\mathcal{A}$	Areas
$\mathcal{E}$	Transmission links
$\mathcal{E}^{\text{From}}_{a}$	Transmission links from area a
$\mathcal{E}^{\text{To}}_{a}$	Transmission links to area a
$\mathcal{L}^{\text{From}}_{n}$	Links from node n
$\mathcal{L}^{\text{To}}_{n}$	Links to node n
$\mathcal{M}_{l}$	Transmission modes on link l
$\mathcal{M}_{lp}$	Transmission modes on link l that transport resource p
$\mathcal{T}^{start}$	First time-step in operational sub-periods
$\mathcal{M}^{\text{Inv}}_{l}$	Transmission modes on link l with investments
$\mathcal{N}^{\text{Cap}}$	Nodes with some production capacity
$\mathcal{N}^{\text{Inv}}$	Nodes with investments available
$\mathcal{N}^{\text{Net}}$	Network nodes
$\mathcal{N}^{\text{Sink}}$	Sink nodes
$\mathcal{N}^{\text{Src}}$	Source nodes
$\mathcal{N}^{\text{Storage}}$	Storage nodes
$\mathcal{P}$	Resources
$\mathcal{P}_{a}$	Resources exchanged to/from area a
$\mathcal{P}^{\text{Emission}}$	Emission related resources
$\mathcal{P}^{\text{In}}_{n}$	Resources into node
$\mathcal{P}^{\text{Out}}_{n}$	Resources out from node
$\mathcal{T}$	Operational periods
$\mathcal{T}^{\text{Inv}}$	Investment periods

Variables

a^{ex}_{atp}	Volume of a product imported or exported to an area
c^{inst}_{nt}	Installed capacity of node
c^{use}_{nt}	Produced units per node
$c^{\text{add}}_{nt^{\text{inv}}}$	Invested capacity
c^{curt}_{nt}	Curtailed energy for an intermittent energy source
$c^{\text{i, current}}_{nt^{\text{inv}}}$	Current installed capacity
$\hat{c}^{\text{inv}}_{nt^{\text{inv}}}$	Whether an investment is done (binary variable)
$c^{\text{trans,add}}_{lmt^{\text{inv}}}$	Invested transmission capacity
$c^{\text{trans, current}}_{lmt^{\text{inv}}}$	Current installed transmission capacity
$\hat{c}^{\text{trans}}_{lmt^{\text{inv}}}$	Whether a transmission investment is done (binary variable)
d^{deficit}_{nt}	Deficit for sink nodes
d^{surplus}_{nt}	Surplus for sink nodes
e_{ntp}	Emissions from node
$e^{\text{strat}}_{i^{\text{inv}}p}$	Total emissions in a strategic period
e^{tot}_{tp}	Total emissions from all nodes in a operational period
f^{in}_{ntp}	Flow into node
f^{out}_{ntp}	Flow out of node
g^{cap}_{ltm}	Transport capacity of a mode
g^{in}_{ltm}	Volume into a transport mode
g^{loss}_{ltm}	Transport loss of a mode
$g^{\text{loss-}}_{ltm}$	Transport loss of a bidirectional mode in opposite direction
$g^{\text{loss+}}_{ltm}$	Transport loss of a bidirectional mode in main direction
g^{out}_{ltm}	Volume out of a transport mode
$h^{\text{acc,use}}_{nt}$	The accumulated use of a hydro storage
h^{tank}_{nt}	Slack variable used for hydro storage
$l^{\text{cap,inst}}_{ltm}$	Pipeline linepack storage capacity
l^{stored}_{ltm}	Pipeline linepack storage level
l^{in}_{ltp}	Flow into of link
l^{out}_{ltp}	Flow out of link
$o^{\text{fix}}_{nt^{\text{inv}}}$	Fixed operational costs
$o^{\text{var}}_{nt^{\text{inv}}}$	Variable operational costs
$s^{\text{cap,inst}}_{nt}$	Installed storage capacity of node
s_{nt}	Storage level
$s^{\text{rate,inst}}_{nt}$	Installed power of storage
$s^{\text{rate,use}}_{nt}$	Storage rate used
$x^{\text{capex,cap}}_{nt^{\text{inv}}}$	CAPEX cost per invested unit
$x^{\text{trans}}_{lmt^{\text{inv}}}$	CAPEX cost per invested transmission capacity

Appendix B. Optimisation model

B.1. Technology representation in the base package

The capacity expansion model is developed in Julia. The design of the program depends on the multiple dispatch feature, with an aim at making the model flexible and easy to extend by others. The model can handle multiple resources or energy carriers, referred to as resources. The programming user interface is based on setting up the energy system as a connected graph. In this setting, the nodes represent either sources, sinks, storages or generation nodes. Generation nodes convert input resources to output resources in some way. Links between the nodes define where the resources can flow. The core package provides a base implementation of the technology nodes. More detailed technology descriptions are implemented in other packages. The division of the model into multiple packages makes the model more comprehensible. This makes it simpler for others to develop new technology nodes fitting their modelling needs.

All nodes except sources and sinks have a link l both in and out. The flow of resources p between nodes is decided by the two constraints (B.1) and (B.2).

$$f^{\text{out}}_{ntp} = \sum_{l \in \mathcal{L}^{\text{From}}_{n}} l^{\text{in}}_{ltp} \qquad n \in \mathcal{N} \setminus \mathcal{N}^{\text{Sink}}, t \in \mathcal{T}, p \in \mathcal{P} \tag{B.1}$$

$$f^{\text{in}}_{ntp} = \sum_{l \in \mathcal{L}^{\text{To}}_{n}} l^{\text{out}}_{ltp} \qquad n \in \mathcal{N} \setminus \mathcal{N}^{\text{Src}}, t \in \mathcal{T}, p \in \mathcal{P} \tag{B.2}$$

Furthermore, the flow of resources into a link is equal to the flow out of the same link, described by (B.3).

$$l^{\text{in}}_{ltp} = l^{\text{out}}_{ltp} \quad l \in \mathcal{L}, t \in \mathcal{T} \tag{B.3}$$

Fixed OPEX is accounted for non-storage (B.4) and storage nodes (B.5) as follows,

$$o^{\text{fix}}_{nt^{\text{inv}}} = O^{\text{fix}}_{nt^{\text{inv}}} c^{\text{inst}}_{n,t^{\text{inv}}_0} \qquad n \in \mathcal{N}, t^{\text{inv}} \in \mathcal{T}^{\text{Inv}} \tag{B.4}$$

$$o^{\text{fix}}_{nt^{\text{inv}}} = O^{\text{fix}}_{nt^{\text{inv}}} s^{\text{cap,inst}}_{n,t^{\text{inv}}_0} \qquad n \in \mathcal{N}^{\text{Storage}}, t^{\text{inv}} \in \mathcal{T}^{\text{Inv}} \tag{B.5}$$

B.1.1. Technology nodes

Network. Let a network node be any node that is neither a source node nor a sink node. The set of network nodes is thus defined as $\mathcal{N}^{\text{Net}} = \mathcal{N} \setminus (\mathcal{N}^{\text{Src}} \cup \mathcal{N}^{\text{Sink}})$. The formulation of the network nodes are described in (B.6) to (B.12) for all network nodes $n \in \mathcal{N}^{\text{Net}}$ and operational times $t \in \mathcal{T}$. The flow of resources into the network node equals the production rate of the network and the per unit utilisation rate of each resource, P^{in}_{np} as stated in (B.6) and similarly for resources flowing out of the network node in (B.7). The production rate of the network node is limited by the installed capacity (B.8).

$$f^{\text{in}}_{ntp} = c^{\text{use}}_{nt} P^{\text{in}}_{np} \qquad p \in \mathcal{P}^{\text{In}}_n \tag{B.6}$$

$$f^{\text{out}}_{ntp} = c^{\text{use}}_{nt} P^{\text{out}}_{np} \qquad p \in \mathcal{P}^{\text{Out}}_n \setminus \{\text{CO}_2\} \tag{B.7}$$

$$c^{\text{use}}_{nt} \leqslant c^{\text{inst}}_{nt} \tag{B.8}$$

The captured CO_2 flowing out from the node is dependent on the capture rates, R^{Capture}_n, and carbon intensity E^{Int}_p of all in-flowing resources (B.9). CO_2 emissions from input resources that are not captured are emitted (B.10). Other emission resources are emitted as no capture technology is implemented (B.11).

$$f^{\text{out}}_{ntp} = R^{\text{Capture}}_n \sum_{\hat{p} \in \mathcal{P}^{\text{In}}_n} E^{\text{Int}}_{\hat{p}} f^{\text{in}}_{nt\hat{p}} \qquad p = \text{CO}_2 \tag{B.9}$$

$$e_{ntp} = (1 - R^{\text{Capture}}_n) \sum_{\hat{p} \in \mathcal{P}^{\text{In}}_n} E^{\text{Int}}_{\hat{p}} f^{\text{in}}_{nt\hat{p}} \qquad p = \text{CO}_2 \tag{B.10}$$

$$e_{ntp} = E_{np} c^{\text{use}}_{nt} \qquad p \in \mathcal{P}^{\text{Emission}} \tag{B.11}$$

The total variable OPEX during the operational times is calculated based on the OPEX rate, time step duration and production rate (B.12).

$$o^{\text{var}}_{nt^{\text{inv}}} = \sum_{t \in t^{\text{inv}}} O^{\text{var}}_{nt} c^{\text{use}}_{nt} \Delta t \quad n \in \mathcal{N}^{\text{Net}}, t^{\text{inv}} \in \mathcal{T}^{\text{Inv}} \tag{B.12}$$

Capacity variables for nodes that are not available for new investments are set to the initial capacity in (B.13).

$$c^{\text{inst}}_{nt} = C^{\text{Init}}_{nt} \quad n \in \mathcal{N}^{\text{Cap}} \setminus \mathcal{N}^{\text{Inv}}, t \in \mathcal{T} \tag{B.13}$$

Source. Source nodes can represent inputs of resources into the system such as natural gas from gas fields or exogenous gas markets, or electricity from exogenous electricity markets. Outflow for all source nodes $n \in \mathcal{N}^{\text{Src}}$ and all times $t \in \mathcal{T}$ are defined by (B.14), capacity limits (B.15)and emissions accounting (B.16).

$$f^{\text{out}}_{ntp} = P^{\text{out}}_{np} c^{\text{use}}_{nt} \qquad p \in \mathcal{P}^{\text{Out}}_n \tag{B.14}$$

$$c^{\text{use}}_{nt} \leqslant c^{\text{inst}}_{nt} \tag{B.15}$$

$$e_{ntp} = E_{np} c^{\text{use}}_{nt} \qquad p \in \mathcal{P}^{\text{Emission}} \tag{B.16}$$

The total variable OPEX accounting for the operational period is summarised in (B.17).

$$o^{\text{var}}_{nt^{\text{inv}}} = \sum_{t \in t^{\text{inv}}} O^{\text{var}}_{nt} c^{\text{use}}_{nt} \Delta t \quad n \in \mathcal{N}^{\text{Src}}, t^{\text{inv}} \in \mathcal{T}^{\text{Inv}} \tag{B.17}$$

Sink. Sink nodes are defined in (B.18) to (B.20) for all sink nodes $n \in \mathcal{N}^{\text{Sink}}$ and times $t \in \mathcal{T}$. They have only inflow (B.18) and no outflow. The capacity limit is replaced with a soft equality constraint (B.19) where surplus and deficits are penalised in the objective function. Emissions are accounted for in the same way as for source nodes (B.20).

$$f^{\text{in}}_{ntp} = c^{\text{use}}_{nt} P^{\text{in}}_{np} \qquad p \in \mathcal{P}^{\text{In}}_n \tag{B.18}$$

$$c^{\text{use}}_{nt} + d^{\text{deficit}}_{nt} = c^{\text{inst}}_{nt} + d^{\text{surplus}}_{nt} \tag{B.19}$$

$$e_{ntp} = E_{np} c^{\text{use}}_{nt} \qquad p \in \mathcal{P}^{\text{Emission}} \tag{B.20}$$

The penalties for sink nodes are summarised by the variable OPEX in (B.21) for all sink nodes $n \in \mathcal{N}^{\text{Sink}}$ and strategic periods $t^{\text{inv}} \in \mathcal{T}^{\text{Inv}}$.

$$o^{\text{var}}_{nt^{\text{inv}}} = \sum_{t \in t^{\text{inv}}} (D^{\text{surplus}}_{nt} d^{\text{surplus}}_{nt} + D^{\text{deficit}}_{nt} d^{\text{deficit}}_{nt}) \Delta t \tag{B.21}$$

B.1.2. System level constraints

Constraints required on the system level are accounting for total emissions for each time-step (B.22) and strategic period (B.23).

$$e^{\text{tot}}_{tp} = \sum_{n \in \mathcal{N}} e_{ntp} \qquad t \in \mathcal{T}, p \in \mathcal{P}^{\text{Emission}} \tag{B.22}$$

$$e^{\text{strat}}_{t^{\text{inv}}p} = \sum_{t \in t^{\text{inv}}} e^{\text{tot}}_{tp} \qquad t^{\text{inv}} \in \mathcal{T}^{\text{Inv}}, p \in \mathcal{P}^{\text{Emission}} \tag{B.23}$$

The objective function is also defined on the system level and accounts for variable and fixed operational costs (B.24),

$$\min \sum_{t^{\text{inv}} \in \mathcal{T}^{\text{Inv}}} \sum_{n \in \mathcal{N}} (o^{\text{var}}_{nt^{\text{inv}}} + o^{\text{fix}}_{nt^{\text{inv}}}) \tag{B.24}$$

B.2. Geography

To establish spatial resolution to the energy model, we define geographical areas. An area a is connected to a core node n in a local energy system consisting of a set of nodes connected by links. Long-distance transport of resources p is defined by setting up transmission links l between the areas. The resources exchanged between the local energy system and other areas, are accounted using the variable a^{ex}_{atp} defined in (B.25) for all areas $a \in \mathcal{A}$, resources in an area $p \in \mathcal{P}_a$ and times $t \in \mathcal{T}$.

$$a^{\text{ex}}_{atp} = f^{\text{in}}_{ntp} - f^{\text{out}}_{ntp} \tag{B.25}$$

For each transport link, we can define one or more transmission modes m. These modes can define different constraints handling the technical details of the resource flow. The balance of resources exchanged is defined in (B.26) for all areas $a \in \mathcal{A}$, resources in an area $p \in \mathcal{P}_a$ and times $t \in \mathcal{T}$.

$$a^{\text{ex}}_{atp} = \sum_{l \in \mathcal{E}^{\text{To}}_a} \sum_{m \in \mathcal{M}_{lp}} g^{\text{in}}_{ltm} - \sum_{l \in \mathcal{E}^{\text{From}}_a} \sum_{m \in \mathcal{M}_{lp}} g^{\text{out}}_{ltm} \tag{B.26}$$

B.2.1. Transmission modes

The transmission modes are defined in (B.27) to (B.33) for all transmission links $l \in \mathcal{E}$, transmission modes on a transmission link $m \in \mathcal{M}_l$ and operational times $t \in \mathcal{T}$. The resource flow in a reference transmission mode m is defined by (B.27), and the output transmission capacity is bonded by g^{cap}_{ltm} in (B.28).

$$g^{\text{out}}_{ltm} = g^{\text{in}}_{ltm} - g^{\text{loss}}_{ltm} \tag{B.27}$$

$$g^{\text{out}}_{ltm} \leqslant g^{\text{cap}}_{ltm} \tag{B.28}$$

For a unidirectional transport mode, the transmission loss is proportional to the transmission input g^{in}_{ltm} (B.29), and the output is required to be non-negative (B.30).

$$g^{\text{loss}}_{ltm} = T^{\text{loss}}_m g^{\text{in}}_{ltm} \tag{B.29}$$

$$g^{\text{out}}_{ltm} \geqslant 0 \tag{B.30}$$

For a bidirectional transport mode, flow in the opposite direction is described by a negative sign, with a lower bound (B.31). The definitions of the transmission loss take the bidirectional flow into account in (B.32) and (B.33).

$$g^{\text{in}}_{ltm} \geqslant -g^{\text{cap}}_{ltm} \tag{B.31}$$

$$g^{\text{loss}}_{ltm} = g^{\text{loss+}}_{ltm} + g^{\text{loss-}}_{ltm} \tag{B.32}$$

Table C.1
Installed and potential capacities for wind farms in the system. The potential for new wind power cites are based on [24] and related source data published on GitHub [38].

Wind farm	Country	Coordinates	Bottom Fixed		Floating	
		(Lon, Lat)	Inst (MW)	Pot (MW)	Inst (MW)	Pot (MW)
Moray Firth	UK	−3.0, 58.2	588	6,588	0	13,974
Firth of Forth	UK	−2.1, 56.4	93	12,636	30	33,294
Dogger Bank	UK	2.3, 54.8	0	19,512	0	0
Hornsea	UK	1.9, 53.8	1,218	14,466	0	0
Outer Dowsing	UK	0.9, 53.8	2,185.5	7,518	0	0
Norfolk	UK	2.2, 52.8	60	9,756	0	0
East Anglia	UK	1.9, 51.9	2,812	8,106	0	0
Borssele	NL	3.2, 52.0	3,739.3	5,858	0	0
Hollandsee Kust	NL	4.0, 52.5	357	7,997	0	0
Helgolander Bucht	DE	7.2, 54.3	7,166	27,493	0	0
Nordsøen	DK	7.0, 56.3	1,120	24,132	0	0
Utsira Nord	NO	4.5, 59.3	0	0	0	6,007
Sørlige NordsjøI	NO	3.6, 57.5	0	4,074	0	4,074
Sørlige NordsjøII	NO	4.9, 56.8	0	2,573	0	12,866

Table C.2
Investment and operational costs for electrolysis [39] and offshore wind technologies [24,38].

Year	Electrolysis			Bottom-fixed Wind			Floating Wind		
	Inv k€/MW	Var OM €/MW h	Fix OM k€/MW	Inv k€/MW	Var OM €/MW h	Fix OM k€/MW	Inv k€/MW	Var OM €/MW h	Fix OM k€/MW
2025	1,291	0.38	48.8	2,778	0.91	94	4,244	0.91	94
2030	807	0.22	45.0	2,048	0.91	94	2,540	0.91	94
2040	591	0.22	33.8	1,929	0.91	94	2,315	0.91	94
2050	482	0.22	22.5	1,891	0.91	94	2,239	0.91	94

Table C.3
Investment data for HVDC lines [14] and H_2 pipelines [35].

Component	Cost	Unit	HVDC cable	H_2 pipe high	H_2 pipe low
Shore node	var	k€/MW	113	–	–
	fix	M€	23.5	–	–
Branch	var cap	€/(MW km)	980	263	536
	var km	M€/km	0.27	–	–
	fix	M€	3.63	–	–
	min cap	GW	0.7	13	4.7
Offshore node	var	k€/MW	723	–	–
	fix	M€	57.3	–	–

$$g_{ltm}^{\text{loss+}} - g_{ltm}^{\text{loss-}} = \frac{1}{2} T_m^{\text{loss}} \left(g_{ltm}^{\text{in}} + g_{ltm}^{\text{out}} \right) \tag{B.33}$$

Capacities are fixed for the existing transmission modes which cannot be invested in $m \in \mathcal{M}_l \setminus \mathcal{M}_l^{\text{Inv}}$ in (B.34).

$$g_{ltm}^{\text{cap}} \leqslant T_m^{\text{cap,init}} \tag{B.34}$$

B.3. Renewable energy

Non-dispatchable intermittent energy sources are implemented similar to a source node, so the constraints (B.14) to (B.17) also holds here. The only difference is the added parameter profile W_{nt}^{profile}. This field is a time series of ratios between 0 and 1, representing the possible maximum available production capacity at a given time as a ratio of the installed capacity. The variable c_{nt}^{curt} represents the curtailment of the energy source, defined by

$$c_{nt}^{\text{use}} + c_{nt}^{\text{curt}} = W_{nt}^{\text{profile}} \cdot c_{nt}^{\text{inst}}, \qquad t \in \mathcal{T}, \tag{B.35}$$

for each intermittent energy source n.

B.4. Investments

B.4.1. Capacity investments

Investments in installed capacity are defined in (B.36) to (B.41) for nodes that allows for investments $n \in \mathcal{N}^{\text{Inv}}$ and all strategic periods $t^{\text{inv}} \in \mathcal{T}^{\text{Inv}}$. The investments are managed with the help variable $c_{nt^{\text{inv}}}^{\text{i, current}}$, set to equal the installed capacity, and bounded above by the max installed capacity (B.36).

$$c_{nt}^{\text{use}} \leqslant c_{nt}^{\text{inst}} = c_{nt^{\text{inv}}}^{\text{i, current}} \leqslant C_{nt^{\text{inv}}}^{\text{max,inst}} t \in t^{\text{inv}} \tag{B.36}$$

The initial installed capacity C_{nt}^{Init} can be increased by investments, using the variable $c_{nt^{\text{inv}}}^{\text{add}}$, in (B.37). A special case is applied for the first strategic period where the initial capacity is set by the initial capacity parameter in (B.38). The parameter $X_{nt^{\text{inv}}}^{\text{capex,cap}}$ describes the cost of each capacity added in (B.39),

$$c_{nt^{\text{inv}}}^{\text{i, current}} = c_{n,t^{\text{inv}}-1}^{\text{i, current}} + c_{nt^{\text{inv}}}^{\text{add}} \qquad t \in t^{\text{inv}} \setminus t_0^{inv} \tag{B.37}$$

$$c_{nt^{\text{inv}}}^{\text{i, current}} = C_{nt}^{\text{Init}} + c_{nt^{\text{inv}}}^{\text{add}} \qquad t^{\text{inv}} = t_0^{inv} \tag{B.38}$$

$$x_{nt^{\text{inv}}}^{\text{capex,cap}} = X_{nt^{\text{inv}}}^{\text{capex,cap}} c_{nt^{\text{inv}}}^{\text{add}} \tag{B.39}$$

Continuous investments. Different investment types require different technical details. Continuous investments have upper and lower bounds for the capacity that can be added in each strategic period,

$$C_{nt^{\text{inv}}}^{\text{min,add}} \leqslant c_{nt^{\text{inv}}}^{\text{add}} \leqslant C_{nt^{\text{inv}}}^{\text{max,add}} \tag{B.40}$$

However, if $C_{nt^{\text{inv}}}^{\text{min,add}}$ is set to a value strictly greater than zero, this will enforce an investment of at least the minimum capacity in each strategic period.

Semicontinuous investments. We now admit a lower bound $C_{nt^{\text{inv}}}^{\text{min,add}} > 0$ for the added capacity, without requiring investment in each period.

This is referred to as semicontinuous investments. This is achieved by multiplying the investment bounds with the binary variable $\hat{c}^{\text{inv}}_{nt^{\text{inv}}}$,

$$C^{\text{min,add}}_{nt^{\text{inv}}} \hat{c}^{\text{inv}}_{nt^{\text{inv}}} \leqslant c^{\text{add}}_{nt^{\text{inv}}} \leqslant C^{\text{max,add}}_{nt^{\text{inv}}} \hat{c}^{\text{inv}}_{nt^{\text{inv}}} \tag{B.41}$$

B.4.2. Transmission investments

Investments in transmission are defined by (B.42) to (B.47) for all lines $l \in \mathcal{E}$, the associated transmission modes $m \in \mathcal{M}^{\text{Inv}}_l$ and all strategic periods $t^{\text{inv}} \in \mathcal{T}^{\text{Inv}}$.

$$g^{\text{cap}}_{ltm} = c^{\text{trans, current}}_{lmt^{\text{inv}}} \tag{B.42}$$

The current transmission capacity at any time depends on the capacity in the previous strategic period and the invested capacities $c^{\text{trans,add}}_{lmt^{\text{inv}}}$ in the current strategic period (B.43). For the first strategic period initial capacity is given in the parameter $T^{\text{cap,init}}_m$ (B.44). The CAPEX of an investment depends on the parameter $X^{\text{capex,trans}}_{lmt^{\text{inv}}}$ and the invested capacity, as shown in (B.45).

$$c^{\text{trans, current}}_{lmt^{\text{inv}}} = c^{\text{trans, current}}_{lm,t^{\text{inv}}-1} + c^{\text{trans,add}}_{lmt^{\text{inv}}} \qquad t \in t^{\text{inv}} \setminus t^{inv}_0 \tag{B.43}$$

$$c^{\text{trans, current}}_{lmt^{\text{inv}}} = T^{\text{cap,init}}_m + c^{\text{trans,add}}_{lmt^{\text{inv}}} \qquad t^{\text{inv}} = t^{inv}_0 \tag{B.44}$$

$$x^{\text{trans}}_{lmt^{\text{inv}}} = X^{\text{capex,trans}}_{lmt^{\text{inv}}} c^{\text{trans,add}}_{lmt^{\text{inv}}} \tag{B.45}$$

As before, the capacity that can be added in an strategic period depends on the investment mode. Continuous and semi-continuous investment modes are described in (B.46) and (B.47), respectively.

$$C^{\text{trans,min,add}}_{lmt^{\text{inv}}} \leqslant c^{\text{trans,add}}_{lmt^{\text{inv}}} \leqslant C^{\text{trans,max,add}}_{lmt^{\text{inv}}} \tag{B.46}$$

$$C^{\text{trans,min,add}}_{lmt^{\text{inv}}} \hat{c}^{\text{trans}}_{lmt^{\text{inv}}} \leqslant c^{\text{trans,add}}_{lmt^{\text{inv}}} \leqslant \hat{c}^{\text{trans}}_{lmt^{\text{inv}}} C^{\text{trans,max,add}}_{lmt^{\text{inv}}} \tag{B.47}$$

B.4.3. Objective function

When investments are used, the objective function is adjusted to optimise the net present value of the fixed and varying operational costs, the investment costs in production and transmission capacity, in addition to the total emission tax cost. The discount factor r is constant, and the objective function is defined as

$$\begin{aligned}\min \sum_{t^{\text{inv}} \in \mathcal{T}^{\text{Inv}}} \left(\frac{1}{1+r}\right)^{t^{\text{inv}}.y} \Bigg(& \sum_{n \in \mathcal{N}^{\text{Cap}}} (o^{\text{var}}_{nt^{\text{inv}}} + O^{\text{fix}}_{nt^{\text{inv}}}) \Delta t^{\text{inv}} \\ & + \sum_{n \in \mathcal{N}^{\text{Inv}}} x^{\text{capex,cap}}_{nt^{\text{inv}}} + \sum_{l \in \mathcal{E}} \sum_{m \in \mathcal{M}_l} x^{\text{trans}}_{lmt^{\text{inv}}} \\ & + \sum_{p \in \mathcal{P}^{\text{Emission}}} E^{\text{cost}}_{pt^{\text{inv}}} e^{\text{strat}}_{t^{\text{inv}}p} \Bigg)\end{aligned} \tag{B.48}$$

In the above, we denote the start year of strategic period t^{inv} by $t^{\text{inv}}.y$, defined as the sum of the length of all preceding strategic periods, that is,

$$t^{\text{inv}}.y = \sum_{t_i < t^{\text{inv}}} \Delta t_i. \tag{B.49}$$

Appendix C. Capacity and investment costs

See Tables C.1–C.3.

References

[1] Shukla P, Skea J, Slade R, Khourdajie AA, van Diemen R, McCollum D, Pathak M, Some S, Vyas P, Fradera R, Belkacemi M, Hasija A, Lisboa G, Luz S, Malley J, editors. IPCC, 2022. In: Climate change 2022: mitigation of climate change. Contribution of working group III to the sixth assessment report of the intergovernmental panel on climate change. Cambridge, UK and New York, NY, USA: Cambridge University Press; 2022, http://dx.doi.org/10.1017/9781009157926.

[2] IEA. Offshore wind outlook 2019. Paris: IEA; 2019, URL: https://www.iea.org/reports/offshore-wind-outlook-2019.

[3] United Nations. Paris agreement. 2015, URL: https://unfccc.int/sites/default/files/resource/parisagreement_publication.pdf.

[4] European Commission. The European green deal. 2019, European Commission, URL: https://eur-lex.europa.eu/legal-content/EN/TXT/?uri=COM%3A2019%3A640%3AFIN.

[5] European Parliament. Council regulation (EU) no P9_TA(2022)0032: A European strategy for offshore renewable energy. Off J Eur Union 2022. URL: https://www.europarl.europa.eu/doceo/document/TA-9-2022-0032_EN.pdf.

[6] Wind Europe Market Intelligence, Ramírez L. Offshore wind energy 2022 mid-year statistics. Technical report, Wind Europe; 2022, URL: https://windeurope.org/intelligence-platform/product/offshore-wind-energy-2022-mid-year-statistics/#overview.

[7] Soares-Ramos E, de Oliveira-Assis L, Sarrias-Mena R, Fernández-Ramírez L. Current status and future trends of offshore wind power in Europe. Energy 2020;202. http://dx.doi.org/10.1016/j.energy.2020.117787.

[8] Pathak M, Slade R, Shukla P, Skea J, Pichs-Madruga R, Ürge-Vorsatz D. Technical Summary. In: Shukla P, Skea J, Slade R, Khourdajie AA, van Diemen R, McCollum D, Pathak M, Some S, Vyas P, Fradera R, Belkacemi M, Hasija A, Lisboa G, Luz S, Malley J, editors. Climate change 2022: mitigation of climate change. Contribution of working group III to the sixth assessment report of the intergovernmental panel on climate change. Cambridge, UK and New York, NY, USA: Cambridge University Press; 2022, p. 65–206. http://dx.doi.org/10.1017/9781009157926.002.

[9] European Commission. An EU Strategy to harness the potential of offshore renewable energy for a climate neutral future. 2020, European Commission, URL: https://eur-lex.europa.eu/legal-content/EN/TXT/?uri=COM%3A2020%3A741%3AFIN, Document Number: COM(2020) 741 final.

[10] Stocks M, Stocks R, Lu B, Cheng C, Blakers A. Global Atlas of closed-loop pumped hydro energy storage. Joule 2021;5(1):270–84. http://dx.doi.org/10.1016/j.joule.2020.11.015.

[11] Davis SJ, Lewis NS, Shaner M, Aggarwal S, Arent D, Azevedo IL, et al. Net-zero emissions energy systems. Science 2018;360(6396):eaas9793. http://dx.doi.org/10.1126/science.aas9793, Publisher: American Association for the Advancement of Science.

[12] International Energy Agency. The future of hydrogen. Technical report, International Energy Agency; 2019, p. 203.

[13] Gonzalez-Rodriguez AG. Review of offshore wind farm cost components. Energy Sustain Dev 2017;37:10–9. http://dx.doi.org/10.1016/j.esd.2016.12.001.

[14] Vrana TK, Härtel P. Estimation of investment model cost parameters for VSC HVDC transmission infrastructure. Electr Power Syst Res 2017;159:98–108. http://dx.doi.org/10.1016/j.epsr.2018.02.007.

[15] Lüth A, Seifert PE, Egging-Bratseth R, Weibezahn J. How to connect energy islands: Trade-offs between hydrogen and electricity infrastructure. Appl Energy 2023;341:121045. http://dx.doi.org/10.1016/j.apenergy.2023.121045.

[16] van Wingerden T, Geerdink D, Taylor C, Hülsen CF. Specification of a European offshore hydrogen backbone. Technical report, DNV; 2023, p. 74, URL: https://www.gascade.de/fileadmin/downloads/DNV-Study_Specification_of_a_European_Offshore_Hydrogen_Backbone.pdf.

[17] Ibrahim OS, Singlitico A, Proskovics R, McDonagh S, Desmond C, Murphy JD. Dedicated large-scale floating offshore wind to hydrogen: Assessing design variables in proposed typologies. Renew Sustain Energy Rev 2022;160:112310. http://dx.doi.org/10.1016/j.rser.2022.112310.

[18] McKenna R, D'Andrea M, González MG. Analysing long-term opportunities for offshore energy system integration in the Danish North Sea. Adv Appl Energy 2021;4. http://dx.doi.org/10.1016/j.adapen.2021.100067.

[19] Svendsen HG. Optimised operation of low-emission offshore oil and gas platform integrated energy systems. 2022, URL: http://arxiv.org/abs/2202.05072, Number: arXiv:2202.05072arXiv:2202.05072 [cs, eess].

[20] Zhang H, Tomasgard A, Knudsen BR, Svendsen HG, Bakker SJ, Grossmann IE. Modelling and analysis of offshore energy hubs. Energy 2022;261:125219. http://dx.doi.org/10.1016/j.energy.2022.125219.

[21] Singlitico A, Østergaard J, Chatzivasileiadis S. Onshore, offshore or in-turbine electrolysis? Techno-economic overview of alternative integration designs for green hydrogen production into Offshore Wind Power Hubs. Renew Sustain Energy Transit 2021;1:100005. http://dx.doi.org/10.1016/j.rset.2021.100005.

[22] McDonagh S, Ahmed S, Desmond C, Murphy JD. Hydrogen from offshore wind: Investor perspective on the profitability of a hybrid system including for curtailment. Appl Energy 2020;265:114732. http://dx.doi.org/10.1016/j.apenergy.2020.114732.

[23] Gea-Bermúdez J, Bramstoft R, Koivisto M, Kitzing L, Ramos A. Going offshore or not: Where to generate hydrogen in future integrated energy systems? Energy Policy 2023;174:113382. http://dx.doi.org/10.1016/j.enpol.2022.113382.

[24] Durakovic G, del Granado PC, Tomasgard A. Powering Europe with North Sea offshore wind: The impact of hydrogen investments on grid infrastructure and power prices. Energy 2023;263:125654. http://dx.doi.org/10.1016/j.energy.2022.125654.

[25] Scolaro M, Kittner N. Optimizing hybrid offshore wind farms for cost-competitive hydrogen production in Germany. Int J Hydrogen Energy 2022;47(10):6478–93. http://dx.doi.org/10.1016/j.ijhydene.2021.12.062.

[26] Gawlick J, Hamacher T. Impact of coupling the electricity and hydrogen sector in a zero-emission European energy system in 2050. Energy Policy 2023;180:113646. http://dx.doi.org/10.1016/j.enpol.2023.113646.

[27] Lucas TR, Ferreira AF, Santos Pereira RB, Alves M. Hydrogen production from the WindFloat Atlantic offshore wind farm: A techno-economic analysis. Appl Energy 2022;310:118481. http://dx.doi.org/10.1016/j.apenergy.2021.118481.

[28] Obara S, Li J. Evaluation of the introduction of a hydrogen supply chain using a conventional gas pipeline–A case study of the Qinghai–Shanghai hydrogen supply chain. Int J Hydrogen Energy 2020;45(58):33846–59. http://dx.doi.org/10.1016/j.ijhydene.2020.09.009.

[29] Sens L, Piguel Y, Neuling U, Timmerberg S, Wilbrand K, Kaltschmitt M. Cost minimized hydrogen from solar and wind – Production and supply in the European catchment area. Energy Convers Manage 2022;265:115742. http://dx.doi.org/10.1016/j.enconman.2022.115742.

[30] Klatzer T, Bachhiesl U, Wogrin S. State-of-the-art expansion planning of integrated power, natural gas, and hydrogen systems. Int J Hydrogen Energy 2022;47(47):20585–603. http://dx.doi.org/10.1016/j.ijhydene.2022.04.293.

[31] He G, Mallapragada DS, Bose A, Heuberger CF, Gençer E. Hydrogen supply chain planning with flexible transmission and storage scheduling. IEEE Trans Sustain Energy 2021;12(3):1730–40. http://dx.doi.org/10.1109/TSTE.2021.3064015.

[32] Quarton CJ, Samsatli S. Should we inject hydrogen into gas grids? Practicalities and whole-system value chain optimisation. Appl Energy 2020;275:115172. http://dx.doi.org/10.1016/j.apenergy.2020.115172.

[33] Dunning I, Huchette J, Lubin M. JuMP: A modeling language for mathematical optimization. SIAM Rev 2017;59(2):295–320. http://dx.doi.org/10.1137/15M1020575.

[34] Backe S, Skar C, del Granado PC, Turgut O, Tomasgard A. EMPIRE: An open-source model based on multi-horizon programming for energy transition analyses. SoftwareX 2022;17:100877. http://dx.doi.org/10.1016/j.softx.2021.100877.

[35] Jens J, Wang A, van der Leun K, Peters D, Buseman M. Extending the European hydrogen backbone, april. 2021, p. 32.

[36] Haeseldonckx D, D'haeseleer W. The use of the natural-gas pipeline infrastructure for hydrogen transport in a changing market structure. In: EHEC2005, Int J Hydrogen Energy In: EHEC2005, 2007;32(10):1381–6.http://dx.doi.org/10.1016/j.ijhydene.2006.10.018,

[37] Haeseldonckx D, D'haeseleer W. Concrete transition issues towards a fully-fledged use of hydrogen as an energy carrier: Methodology and modelling. Int J Hydrogen Energy 2011;36(8):4636–52. http://dx.doi.org/10.1016/j.ijhydene.2011.01.113.

[38] OpenEMPIRE. 2023, NTNU, URL: https://github.com/Goggien/EMPIRE-Public. [Accessed: 28 March 2023].

[39] Seck GS, Hache E, Sabathier J, Guedes F, Reigstad GA, Straus J, et al. Hydrogen and the decarbonization of the energy system in Europe in 2050: A detailed model-based analysis. Renew Sustain Energy Rev 2022;167:112779. http://dx.doi.org/10.1016/j.rser.2022.112779.